Contrib Mineral Petrol (2011) 161:13–33
DOI 10.1007/s00410-010-0519-x

ORIGINAL PAPER

Uniformly mantle-like $\delta^{18}O$ in zircons from oceanic plagiogranites and gabbros

Craig B. Grimes · Takayuki Ushikubo · Barbara E. John · John W. Valley

Received: 8 December 2009 / Accepted: 30 March 2010 / Published online: 24 April 2010

Abstract Lower ocean crust is primarily gabbroic, although 1–2% felsic igneous rocks that are referred to collectively as plagiogranites occur locally. Recent experimental evidence suggests that plagiogranite magmas can form by hydrous partial melting of gabbro triggered by seawater-derived fluids, and thus they may indicate early, high-temperature hydrothermal fluid circulation. To explore seawater–rock interaction prior to and during the genesis of plagiogranite and other late-stage magmas, oxygen-isotope ratios preserved in igneous zircon have been measured by ion microprobe. A total of 197 zircons from 43 plagiogranite, evolved gabbro, and hydrothermally altered fault rock samples have been analyzed. Samples originate primarily from drill core acquired during Ocean Drilling Program and Integrated Ocean Drilling Program operations near the Mid-Atlantic and Southwest Indian Ridges. With the exception of rare, distinctively luminescent rims, all zircons from ocean crust record remarkably uniform $\delta^{18}O$ with an average value of 5.2 ± 0.5‰ (2SD). The average $\delta^{18}O$(Zrc) would be in magmatic equilibrium with unaltered MORB [$\delta^{18}O$(WR) ~ 5.6–5.7‰], and is consistent with the previously determined value for equilibrium with the mantle. The narrow range of measured $\delta^{18}O$ values is predicted for zircon crystallization from variable parent melt compositions and temperatures in a closed system, and provides no indication of any interactions between altered rocks or seawater and the evolved parent melts. If plagiogranite forms by hydrous partial melting, the uniform mantle-like $\delta^{18}O$(Zrc) requires melting and zircon crystallization prior to significant amounts of water–rock interactions that alter the protolith $\delta^{18}O$. Zircons from ocean crust have been proposed as a tectonic analog for >3.9 Ga detrital zircons from the earliest (Hadean) Earth by multiple workers. However, zircons from ocean crust are readily distinguished geochemically from zircons formed in continental crustal environments. Many of the >3.9 Ga zircons have mildly elevated $\delta^{18}O$ (6.0–7.5‰), but such values have not been identified in any zircons from the large sample suite examined here. The difference in $\delta^{18}O$, in combination with newly acquired lithium concentrations and published trace element data, clearly shows that the >3.9 Ga detrital zircons did not originate by processes analogous to those in modern mid-ocean ridge settings.

Keywords Zircon · Oxygen isotopes · SIMS · Plagiogranite · Ocean crust · Hadean

Communicated by J. Hoefs.

Electronic supplementary material The online version of this article (doi:10.1007/s00410-010-0519-x) contains supplementary material, which is available to authorized users.

C. B. Grimes (✉) · T. Ushikubo · J. W. Valley
Department of Geoscience, WiscSIMS, University of Wisconsin, 1215W. Dayton St., Madison, WI 53706, USA
e-mail: cgrimes@geosci.msstate.edu

B. E. John
Department of Geology and Geophysics, University of Wyoming, Laramie, WY 82071, USA

Present Address:
C. B. Grimes
Department of Geosciences, Mississippi State University, Mississippi State, MS 39762-5448, USA

Introduction

The circulation of seawater beneath mid-ocean ridges (MORs) can lead to pervasive alteration of ocean crust, and

facilitates significant heat and elemental fluxes (e.g., Gregory and Taylor 1981; Muehlenbachs 1986; McCaig et al. 2010). Studies of lower (gabbroic) ocean crust formed at both fast and slow spreading rates indicate that the onset of brittle fracturing and penetration of seawater-derived hydrothermal fluids may occur at temperatures of 600–750°C based on geochemistry of amphibole filling early fractures and oxygen isotope data (e.g., Stakes et al. 1991; Gillis 1995; Manning et al. 1996). Hydrothermal alteration at even higher temperatures up to 900°C has been proposed based largely on thermometry of coexisting brown amphibole–plagioclase pairs (Gaggero and Cortesogno 1997; Manning et al. 2000; Maeda et al. 2002; Nicolas et al. 2003; Bosch et al. 2004). McCollom and Shock (1998) noted that seawater circulation occurring at 750–900°C would leave little to no mineralogical expression, and could thus be more extensive than is typically concluded from mineralogical studies. The high temperatures reported for hydrothermal alteration approach and even exceed the wet solidus of lower crustal gabbros (Dixon-Spulber and Rutherford 1983; Coogan et al. 2001; Koepke et al. 2004). Thus, early infiltration of seawater, or reheating/melting of hydrothermally altered gabbro may have a significant, although as yet incompletely understood impact on late-stage magmatic processes in MOR settings.

As the most differentiated and latest-stage magmas in ocean crust, oceanic plagiogranite is likely to record evidence of early, high-temperature infiltration of seawater-derived hydrothermal fluids. The term *plagiogranite* is used broadly here to reference the suite of felsic plutonic rocks (i.e., anorthosite, diorite, quartz diorite, and tonalite/trondjhemite) found in modern ocean crust and ophiolites (e.g., Coleman and Donato 1979), including the 'felsic dikes', 'felsic segregations', and 'late leucocratic magmatic dikelets' described from Ocean Drilling Program (ODP) Hole 735B (57°E, southwest Indian Ridge) and Integrated Ocean Drilling Program (IODP) Hole 1309D (30°N, Mid-Atlantic Ridge) (Dick et al. 2000; Blackman et al. 2006).

Although volumetrically minor (typically $\sim$1–2%), plagiogranite is ubiquitous throughout plutonic ocean crust. These rock types have recently been considered as a potentially significant component of the bulk trace element budget (Hart et al. 1999; Godard et al. 2009), and commonly host uranium-bearing minerals (i.e. zircon) amenable to radiometric dating (John et al. 2004; Schwartz et al. 2005; Grimes et al. 2008; Baines et al. 2009). Moreover, plagiogranites formed beneath MORs by melting of hydrothermally altered mafic crust have been hypothesized as analogs to parental magmas of 4.4–4.0 Ga detrital zircons, suggesting that the crust on Earth before 4 Ga was primitive and dominantly mafic (Rollinson 2008). Oceanic plagiogranite, therefore, has a significant role in understanding both modern and ancient crustal growth processes.

The origin of oceanic plagiogranite is controversial and has been attributed to a wide variety of processes, including (1) extreme fractional crystallization of MORB, (2) liquid immiscibility with Fe-enriched tholeiitic melts, and (3) hydrous partial melting of oceanic gabbros (review by Koepke et al. 2007). All of these hypotheses have been proposed for plagiogranite from the same location in ODP Hole 735B (Natland et al. 1991; Dick et al. 2000; Natland and Dick 2002; Niu et al. 2002; Koepke et al. 2004), highlighting complexity in discerning mechanisms of formation. Most recently, Koepke et al. (2004, 2007) have presented several lines of geochemical evidence supporting an origin by hydrous partial melting. In slow spreading ocean crust, it is proposed that seawater-derived fluids penetrate the lower crust along deep-rooting detachment fault systems and trigger partial melting (Koepke et al. 2007; Jöns et al. 2009).

Oxygen-isotope ratios are sensitive indicators of the extent and temperature of interactions between seawater and crustal rocks. However, determining magmatic oxygen-isotope ratios is complicated by the fact that whole rocks and most constituent minerals in ocean crust are highly susceptible to sub-solidus exchange and recrystallization during hydrothermal fluid circulation. Thus, evidence of early (magmatic) events tends to be partly or fully overprinted by later (hydrothermal) events at lower temperatures. For gabbro that is infiltrated by seawater, temperature-dependant exchange leads to higher δ^{18}O(WR) >6‰ during water–rock interaction below 200–250°C, and lower δ^{18}O(WR) <5‰ above 200–250°C (e.g., Muehlenbachs 1986; Alt and Bach 2006). Fresh olivine phenocrysts are commonly used to monitor magmatic δ^{18}O values in mafic and ultramafic rocks (Mattey et al. 1994; Eiler et al. 1996; Eiler 2001; Gao et al. 2006; Bindeman et al. 2008), however, olivine is absent from plagiogranite and many other evolved rock types. In contrast, zircons often occur in differentiated rock types within ocean crust. Zircons are also highly resistant to alteration, and commonly preserve primary magmatic δ^{18}O (Valley et al. 1994, 2005; Valley 2003; Page et al. 2007a). The ability to correlate age concordance and Pb-loss to δ^{18}O(Zrc) readily identifies altered zircon and makes determinations of magmatic chemistry from zircon uniquely reliable. Thus, igneous zircons provide a means for tracking magmatic δ^{18}O values of plagiogranite and other late-stage, differentiated rock types.

In a previous ion microprobe study of 24 zircon grains from three gabbro and serpentinite samples collected near the MARK area, 23°N, Mid-Atlantic Ridge (MAR), Cavosie et al. (2009) report an average $\delta^{18}O = 5.3 \pm 0.8$‰, which is indistinguishable from the value in high temperature equilibrium with mantle (5.3 ± 0.6‰; Valley et al. 1998, 2005). In the current study, we present δ^{18}O values of

zircons hosted by an additional 43 rock samples including 23 plagiogranites, 13 gabbros, and 7 serpentinite/fault schists collected from multiple geographic locations and depths along the MAR and Southwest Indian Ridge (SWIR) (Fig. 1). The primary objectives are to constrain magmatic $\delta^{18}O$ of plagiogranite and evolved Fe–Ti oxide gabbro recovered from ocean crust, and to evaluate the timing and extent of high-temperature alteration involving seawater-derived fluids relative to formation and crystallization of these latest-stage magmas. In addition, our results provide a comprehensive framework for interpreting detrital, xenocrystic, and eclogitic zircons potentially originating in a setting similar to modern MORs. Using these new data, we revisit the hypothesis that oceanic plagiogranite could serve as an analog for the Earth's first 'felsic' crust that produced >3.9 Ga Jack Hills detrital Hadean zircons (e.g., Rollinson 2008).

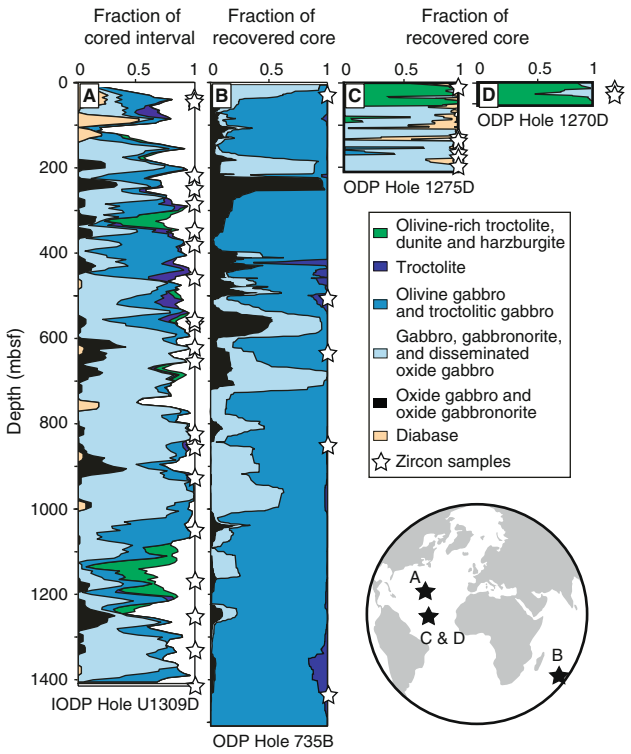

Fig. 1 Stratigraphic distributions of lithologic proportions recovered in ocean drill cores that were sampled for zircons in this study (mbsf = meters below seafloor). The depths of rock samples hosting zircons analyzed for $\delta^{18}O$ are indicated. *A* IODP Hole U1309D, 30°N, Mid-Atlantic Ridge (MAR) (20 m running average of cored interval—*white area* represents no recovery; after Blackman et al. 2006). *B* ODP Hole 735B, 57° E, Southwest Indian Ridge (20 m running average of recovered core; after Dick et al. 2000). *C* ODP Hole 1275D, 15°44′N, MAR and *D* 1270D, 14°43′N, MAR (5 m running average of recovered cores; modified from Kelemen et al. 2004). The geographic locations of the holes represented by *columns A–D* are indicated on the *map* (*lower right*). General rock types for samples hosting zircon are given in Table 1

Geologic setting and sampling

This study incorporates rocks collected along the northern MAR and the SWIR—slow and ultraslow spreading MOR systems with full-spreading rates of ~25 and ~14 mm/year, respectively. In these settings, magmatic events may be episodic and short-lived, with a significant component of plate separation (up to 50% in some segments) accommodated by detachment faulting (e.g., Tucholke et al. 1998; Schroeder et al. 2007; Smith et al. 2008). Detachment fault systems can initiate up to ~7–8 km below the ridge axial valley floor and accommodate tens of kilometers of slip, exposing lower crustal gabbro and mantle peridotite directly on the seafloor (e.g., Tucholke and Lin 1994; Tucholke et al. 1998; Cann et al. 1997; deMartin et al. 2007). The crustal architecture associated with slow spreading ocean crust is thus variable and can differ substantially from the classical layered ophiolite model (e.g., Cannat 1996; Karson 1998; Dick et al. 2000). Seismic studies along the MAR have shown that detachment faults and axial valley bounding faults can extend near or even below zones of partial melt at depths of ~3–7 km (Singh et al. 2006; deMartin et al. 2007), highlighting the potential for dynamic interactions between magmatic, tectonic, and hydrothermal systems during crustal accretion. Taken with mineralogical and textural evidence of extensive recrystallization, Sr and O isotope evidence from whole-rock samples indicate that the detachment faults served as loci for extensive seawater-derived hydrothermal fluid migration (Stakes et al. 1991; McCaig et al. 2007, 2010; Delacour et al. 2008; Jöns et al. 2009). However, the depths and temperatures at which detachment faults are able to act as effective fluid pathways, and the timing of fluid flow are still under investigation.

Thirty-eight rock samples in this study originate from core recovered during ODP and IODP drilling near 57°E, SWIR (Holes 735B and 1105A), 15°N, MAR (Holes 1270D and 1275D), and 30°N, MAR (Holes U1309B and U1309D) (Fig. 1; Table 1). These holes were drilled into the footwalls to oceanic detachment faults, and recovered predominantly gabbroic rocks with minor ultramafic lithologies, diabase, and plagiogranite. An additional five samples in this study were recovered by submersible and dredge from the southern wall of Atlantis Massif (30°N, MAR) during the MARVEL2000 cruise of the R/V Atlantis (Blackman et al. 2004; see Grimes et al. 2008). The crustal age of the sampling locations ranges from 1 to 13 Ma. Sampling provides coverage extending from the seafloor (corresponding to the detachment fault scarp) to 1,430 m below the seafloor in largely intact footwall blocks (Fig. 1).

Table 1 Summary of $\delta^{18}O$ and Ti-in-zircon temperature measured by ion microprobe in magmatic ocean-crust zircons and luminescent (CL) zircon rims (regular pits) from the Mid-Atlantic (MAR) and southwest Indian Ridges (SWIR)

Number	Location/sample (cruise or Leg/Exp-Site-Hole-core, top)	Depth (mbsf)	General rock type[a]	$\delta^{18}O$ (‰, SMOW)[b]						Ti-in-Zrc T (°C, uncorr)[c]		
				Ave.	2SD	2SE	Max	Min	Number of grains	Ave.	2SD	Number of grains
15°N area, MAR (15-28 km off-axis)												
1	209-1270D-3R-1, 47 cm	19	V/D	5.5	0.3	0.1	5.7	5.3	10	803	96	6
2	209-1270D-4R-1, 133 cm	25	V/D	5.2	0.4	0.2	5.5	5.0	5	840	29	7
Average				5.4	0.4				15			
3	209-1275D-2R-2, 96 cm	10	Plgt	5.3	0.4	0.2	5.6	5.0	5	817	60	7
4	209-1275D-29R-2, 89 cm	134	Plgt	5.4	0.5	0.2	5.7	5.1	5			
5	209-1275D-31R-2, 68 cm	144	Plgt	5.3	0.4	0.2	5.5	5.2	3			
6	209-1275D-36R-1, 81 cm	167	Plgt	5.1	0.7	0.4	5.6	4.9	4			
7	209-1275D-39R-2, 0 cm	180	Plgt	5.5	0.2	0.1	5.6	5.4	3			
8	209-1275D-43R-1, 34 cm	200	Plgt	5.5	0.3	0.2	5.6	5.4	2			
Average				5.3	0.5				22			
30°N, MAR (~ 7–14-km off-axis)												
Atlantis Massif (southern wall)												
9	MARVEL2000, *Alvin* 3652-1333	0	FS(OxGb?)	5.1	0.4	0.2	5.4	5.0	3	784	35	6
10	MARVEL2000, *Alvin* 3646-1205	0	FS	5.2	0.3	0.1	5.3	5.1	3	848	52	5
11	MARVEL2000, D3-21 (dredge)	0	FS	5.4	0.5	0.2	5.7	5.1	5	865	69	6
12	MARVEL2000, *Alvin* 3647-1359	0	FS	5.5	0.2	0.1	5.5	5.4	3	829	117	6
13	MARVEL2000, *Alvin* 3652-1002	0	Br	5.6	0.3	0.2	5.7	5.4	2			
Average				5.3	0.4				16			
U1309B and U1309D												
14	304-U1309B-7R-1, 0 cm	38	Plgt	5.1	0.4	0.2	5.3	4.9	5			
15	304-U1309B-7R-1, 77 cm	39	Plgt	4.9	0.2	0.1	5.1	4.8	5	744	32	4
16	304-U1309B-13R-2, 26 cm	68	Plgt	5.2	0.2	0.1	5.3	5.2	3			
17	304-U1309D-5R-3, 136 cm	40	Plgt	5.1	0.3	0.1	5.3	4.8	11	731	40	8
18	304-U1309D-9R-2, 97 cm	58	Plgt	5.2	0.2	0.1	5.4	5.1	4			
19	304-U1309D-40R-1, 21 cm	215	Plgt	5.3	0.2	0.1	5.4	5.2	5	721	35	14
20	305-U1309D-93R-1, 27 cm	463	Plgt	5.3	0.1	0.1	5.3	5.2	4	753	82	10
21	305-U1309D-115R-2, 59 cm	570	Plgt	5.2	0.8	0.3	5.8	4.8	5			
22	305-U1309D-178R-1, 97 cm	867	Plgt	5.2	0.2	0.1	5.3	5.2	3			
23	305-U1309D-216R-1, 54 cm	1,040	Plgt	5.0	0.5	0.2	5.4	4.8	8			
24	305-U1309D-295R-3, 100 cm	1,415	Plgt	5.1	0.3	0.1	5.3	4.8	6	786	69	8
Average				5.2	0.4				59			
25	304-U1309D-47R-2, 102 cm	250	OxGb	5.3	0.3	0.2	5.4	5.0	4			
26	304-U1309D-54R-1, 52 cm	282	OxGb	5.1	0.3	0.2	5.3	4.9	4			
27	304-U1309D-69R-2, 52 cm	355	OxGb	4.9	0.4	0.2	5.1	4.6	5			
28	304-U1309D-75R-3, 99 cm	386	OxGb	5.0	0.3	0.1	5.2	4.8	5			
29	305-U1309D-114R-1, 62 cm	564	OxGb	5.3	0.3	0.2	5.4	5.1	3			
30	305-U1309D-126R-2, 27 cm	623	OxGb	5.0	0.2	0.1	5.1	4.9	4			
31	305-U1309D-131R-2, 0 cm	647	OxGb	5.3	0.2	0.1	5.4	5.2	7	708	31	5
32	305-U1309D-168R-2, 0 cm	820	OxGb	5.2	0.2	0.1	5.3	5.1	4			
33	305-U1309D-189R-4, 41 cm	923	OxGb	5.1	0.5	0.3	5.3	4.9	3			
34	305-U1309D-244R-2, 100 cm	1,175	OxGb	5.0	0.5	0.1	5.3	4.7	10			
35	305-U1309D-259R-1, 22 cm	1,245	OxGb	5.0	0.4	0.2	5.3	4.8	3			
36	305-U1309D-276R-1, 34 cm	1,327	OxGb	5.4	0.4	0.2	5.6	5.2	3			

Table 1 continued

Number	Location/sample (cruise or Leg/Exp-Site-Hole-core, top)	Depth (mbsf)	General rock type[a]	$\delta^{18}O$ (‰, SMOW)[b]						Ti-in-Zrc T (°C, uncorr)[c]		
				Ave.	2SD	2SE	Max	Min	Number of grains	Ave.	2SD	Number of grains
Average				5.1	0.4				55			
Luminescent CL rims												
17	304-U1309D-5R-3, 136 cm	40	Plgt	4.8	0.1	0.0	4.8	4.8	3	625	9	4
24	305-U1309D-295R-3, 100 cm	1,415	Plgt	4.7	0.3	0.1	4.9	4.6	4	624	6	2
Average				4.8	0.2							
57°E, SWIR (~100-km-off-axis)												
37	179-1105A-8R-4, 21 cm	57	Plgt	5.6	0.4	0.2	5.8	5.3	3			
38	118-735B-7D-1, 10 cm	26	Plgt	5.1	0.5	0.2	5.4	4.7	7			
39	176-735B-90R-1, 45 cm	508	Plgt	5.4	0.3	0.2	5.6	5.3	3			
40	176-735B-110R-4, 8 cm	638	Plgt	5.2	0.4	0.2	5.5	5.0	3			
41	176-735B-137R-2, 71 cm	854	Plgt	5.4	0.4	0.2	5.6	5.2	4			
42	176-735B-202R-7, 85 cm	1,430	Plgt	5.0	0.3	0.1	5.2	4.8	6			
Average				5.2	0.5				26			
43	118-735B-28R-1, 56 cm	127	Gb	5.3	0.3	0.2	5.5	5.1	4			

V/D vein/dike in serpentinized peridotite, *Plgt* plagiogranite, *OxGb* oxide gabbro, *FS* fault schist, *Br* breccia, *Gb* gabbro

[a] Rock 'types' based on thin section and/or drill core observation

[b] Variability within each rock sample; replicate analyses on single grains were averaged prior to determining rock-averaged values. The analytical uncertainty of individual spot analyses is ±0.3‰ (2SD)

[c] Uncorrected temperatures from Grimes et al. (2009); standard deviation reflects variability within each rock sample

Host rocks and zircons

Zircons from 43 samples of modern ocean crust were analyzed for $\delta^{18}O$. Host rock types include plagiogranite, evolved Fe–Ti oxide-bearing gabbro, highly altered veins/shear zones in serpentinized ultramafic rocks, and fault schists sampled from detachment shear zones (Table 1; see also Grimes et al. 2009). Zircons were separated from whole rocks by mechanical crushing and heavy liquid mineral separation techniques. Crushed sample volumes ranged from 30 to 550 cm^3, and commonly yielded 10s to several 100s of zircon grains. Zircons were handpicked, cast in epoxy grain mounts and polished to their mid-section. Many of these zircons have previously been analyzed for Pb/U age and/or trace element geochemistry by SHRIMP-RG (Grimes et al. 2008, 2009; Baines et al. 2009).

Plagiogranite from in situ ocean crust occurs as thin (mm to several cm wide), leucocratic dikes or vein networks intruding gabbroic host rocks. Primary mineral assemblages include plagioclase, amphibole, and quartz, and often minor to trace amounts of Fe–Ti oxide, biotite, potassium feldspar, titanite, zircon, and/or apatite. These rocks are commonly overprinted by extensive subsolidus hydrothermal alteration of magmatic plagioclase and amphibole to secondary plagioclase, tremolite/actinolite, chlorite, and smectite (Robinson et al. 2002; Niu et al. 2002; Kelemen et al. 2004; Alt and Bach 2006; Blackman et al. 2006). Samples of evolved gabbroic rocks generally consist of plagioclase + clinopyroxene + Fe–Ti oxide + apatite ± amphibole ± orthopyroxene ± titanite ± zircon. Collectively, these samples are characteristic of evolved plutonic rocks in ocean crust (Dick et al. 2000; Blackman et al. 2006). Plagiogranite tends to produce significantly greater abundances of zircons than evolved oxide gabbros from a given rock volume, however, oxide gabbros comprise approximately an order-of-magnitude greater volume of plutonic ocean crust; both rock types are therefore important carriers of zircon in this setting.

Zircons separated from two core samples from ODP Hole 1270D comprising actinolite/tremolite + chlorite veins/shear zones in serpentinite, and five metasomatized fault schists collected from the detachment fault shear zone on Atlantis Massif (dominated by assemblages of amphibole, talc and/or chlorite) have also been investigated. In ODP Hole 1270D, the protolith of equivalent zircon-bearing shear zones is inferred to be plagiogranite (Jöns et al. 2009). Sample 3652-1333 (Table 1) preserves coarse Fe–Ti oxides suggesting that the protolith was an oxide gabbro; however, the composition of melts crystallizing zircons in the remaining fault schist samples from Atlantis Massif is difficult to determine due to the high degree of alteration. In thin sections of less-deformed samples, zircons are always concentrated in discrete mm- to cm-scale veins or

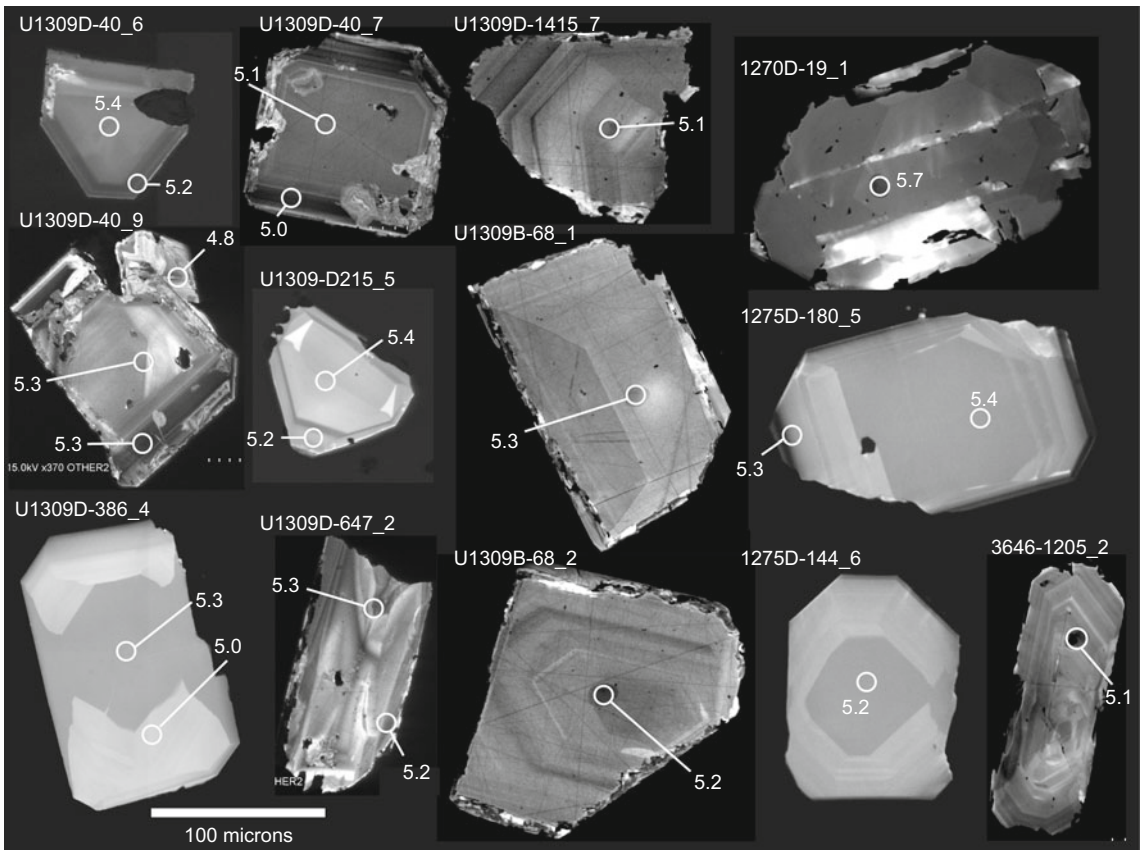

Fig. 2 Representative cathodoluminescence (CL) zoning patterns and ion microprobe analysis spots for $\delta^{18}O$ measurements on normal magmatic ocean-crust zircons (Table 1) from the Mid-Atlantic and Southwest Indian Ridges. Host rocks were collected in place on the seafloor and include plagiogranite, evolved oxide-bearing gabbro, and highly altered serpentinite and fault schist. Many of the zircons in this study have been characterized previously for age (Grimes et al. 2008; Baines et al. 2009) and trace element geochemistry (Grimes et al. 2009)

shear zones dominated by greenschist-facies mineral assemblages (Grimes et al. 2009). These are assumed to reflect intrusions of evolved melt that have been altered.

Representative textures for three types of zircon distinguished by SEM observations and analyzed for $\delta^{18}O$ are shown in Figs. 2 and 3. More than 95% of zircons recovered from ocean-crust rock types resemble typical young igneous zircon, occurring as pristine, clear, colorless grains with oscillatory and sector CL zoning, igneous REE patterns, and magmatic Ti-in-zircon crystallization temperatures (Grimes et al. 2007, 2009; Cavosie et al. 2009). A second type of zircon analyzed for $\delta^{18}O$ is overgrowth rims that are notably luminescent in CL, and yield anomalously lower Ti-in-zircon temperatures (625°C using the uncorrected calibration of Ferry and Watson 2007) in the ocean zircon population (Grimes et al. 2009). Rims wide enough to be analyzed with a ~10 μm spot were found on only seven grains; however, 1–2 μm rims with similar appearance in CL are present on additional grains from both plagiogranite and oxide gabbro. The third type of zircons investigated are distinctly porous, opaque, and faintly colored, often contain mineral inclusions enriched in Y, Th, and U, and CL images reveal perturbed or chaotic zoning ('type 3' from Grimes et al. 2009). Porous domains with perturbed or chaotic zoning cut across relict igneous zones (Fig. 3), implying the porosity is an alteration feature. The porous zircons are not abundant, but are observed in ~25% of the samples studied and occur in both plagiogranites and evolved gabbros. Exploratory analyses were performed on porous zircons from nine different rocks.

Methods

Oxygen isotope measurements

The KIM-5 zircon oxygen isotope standard was face-mounted prior to analysis in the center of pre-existing zircon grain mounts used in this study. The mounts were carefully flattened by hand using 6, 3, and 1 μm diamond lapping film. Progress during flattening was closely monitored under reflected light using an optical microscope, and

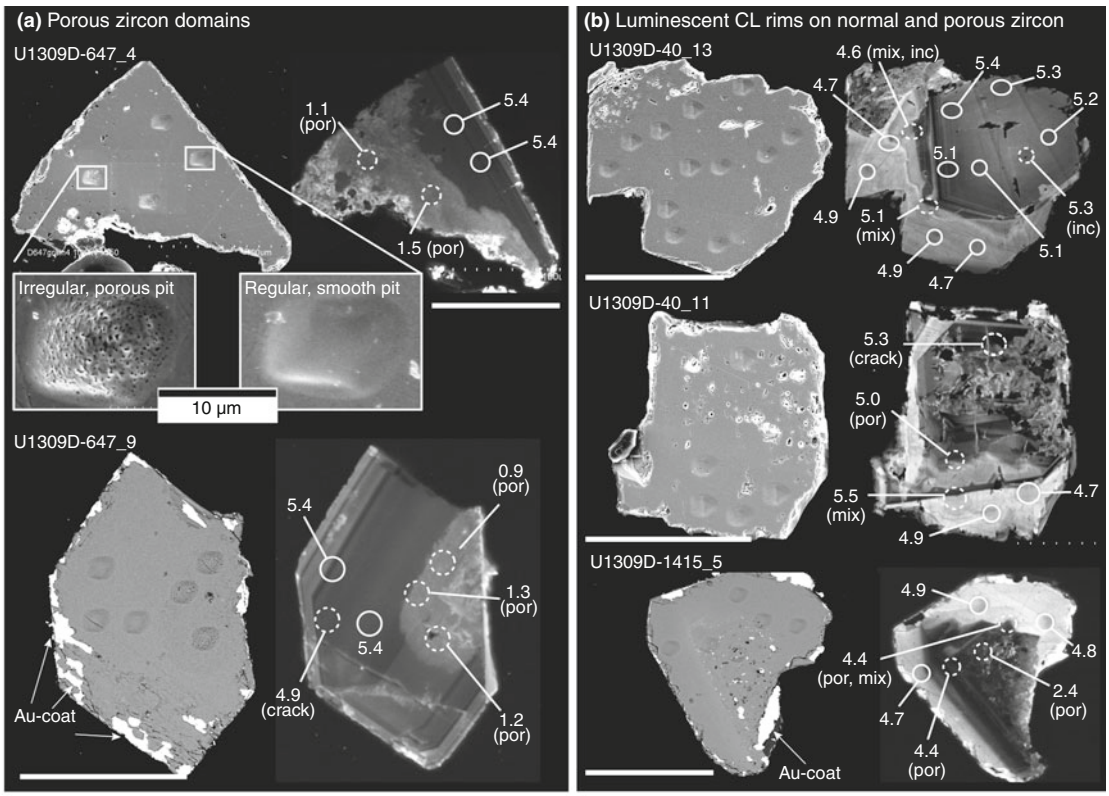

Fig. 3 Representative textures and CL zoning patterns of ocean-crust zircons with **a** porous domains (Table 2) and **b** late, luminescent CL rims (Table 1) (see also Grimes et al. 2009). Analysis spot locations and corresponding $\delta^{18}O$ value are shown. *Dashed spots* indicate irregular pits found to overlap cracks, inclusions, or porous domains that are excluded from average $\delta^{18}O$ values. **a** Matching backscattered electron (BSE *left*) and CL (*right*) images of zircons with porous and non-porous domains. *Inset* enlargement of ion microprobe pits illustrating the contrasting structure of pits located in porous areas versus normal (regular) magmatic zircon domains. Distinctly porous pits are observed in porous zircon domains with perturbed/chaotic CL, whereas smooth-bottomed pits are characteristic of domains exhibiting flat, sector or oscillatory zoning typical of igneous zircon. Sputtering during analysis can preferentially erode and enlarge existing porosity making it more apparent in pit bottoms. **b** Matching BSE (*left*) and CL (*right*) images of representative zircons with luminescent CL rims. '*por*' pits with porous bottoms, '*mix*' spots that overlap multiple CL domains, '*inc*' spots overlapping a mineral inclusion. Residual gold coat (labeled 'Au-coat') is visible on the edges of some grains in BSE images. All *scale bars* 100 µm unless otherwise noted

care was taken to grind the surface of the zircons to a level just below the bottom of the existing pits made during SHRIMP-RG analyses. It has been shown that topographic relief between grains and adjacent epoxy >1 µm, and analyses of spots more than 5 mm from the center of the mount may bias the measured isotopic ratios and degrade spot-to-spot-reproducibility and thus accuracy (Kita et al. 2009). Therefore, after flattening each mount was imaged by Zygo™ optical profilometer at the University of Wisconsin to evaluate relief. The relief on the grain mounts across the areas subsequently analyzed (<6 mm from the center) was less than ~2 µm, and differential relief between individual grains and surrounding epoxy was typically less than 0.5 µm. Zircons were imaged by reflected light, and by cathodoluminescence (CL), and backscattered electrons (BSE) using a Hitachi S-3400N Scanning Electron Microscope (SEM) at the University of Wisconsin to aid in the selection of oxygen isotope analysis spot locations. Mounts were carefully cleaned, dried in a vacuum oven at ~40°C for 1 h, and gold-coated in preparation for SIMS analysis.

Oxygen-isotope ratios were measured using a CAMECA IMS-1280 ion microprobe in the WiscSIMS Laboratory at the University of Wisconsin-Madison, following the procedures outlined by Kita et al. (2009). Analyses were conducted using a focused 1.9–2.2 nA primary Cs^+ beam with a spot size of ~10 µm. Data were acquired during three separate 12-h analytical sessions. Four analyses on zircon standard KIM-5 ($\delta^{18}O = 5.09‰$ VSMOW, Valley 2003) were performed at the beginning of each session, and subsequently after every 10–12 unknowns (Online Resource 1). The average value of the standards bracketing each block of unknowns was used to correct for instrumental bias. The external precision, defined by the spot-to-spot

reproducibility of bracketing standards, is assigned as the measurement uncertainty on individual analyses. The average precision of bracketing standards from all three sessions is ±0.32‰ (2 standard deviations, SD; 2 standard errors = 0.11‰).

After measurement by ion microprobe, the bottoms of all individual analysis pits were imaged by SEM to inspect pit location and structure following the method described by Cavosie et al. (2005). During post-analysis imaging, 33 pits within normal magmatic zircons were identified as 'irregular' on the basis that they encountered cracks or inclusions, or overlapped the grain edge. Data from irregular pits on normal magmatic zircons were rejected, although we note that including these analyses causes the average $\delta^{18}O$ value of the ocean-crust zircon population to decrease by only 0.03‰ while increasing the standard deviation by 0.1‰ (2SD). Thus, the conclusions of this paper would not be affected by including them. Rejected data are included in the supplemental online table (Online Resource 1). Oxygen-isotope ratios are reported in standard delta (δ) notation relative to Vienna standard mean ocean water (VSMOW), and all uncertainties reported in the text, tables, and figures are presented at the 2SD level.

Lithium concentration

The Li concentrations of 31 ocean-crust zircons (33 spots) were analyzed with the WiscSIMS CAMECA IMS-1280 ion microprobe for comparison with the zircon dataset of Ushikubo et al. (2008). Analyses were conducted using an impact energy of 23 keV with Kohler illumination mode, an O^- beam of ~2.8 nA, and a spot size of ~25 μm in diameter. The secondary ions were accelerated at 10 keV and were detected with an axial electron multiplier (mono collection) by magnetic peak switching. The mass resolving power ($M/\Delta M$) was set at ~3,000. Details of other parameters of the secondary-ion optics are described by Ushikubo et al. (2008). Total analysis time was 9 min, consisting of pre-sputtering (240 s), beam centering (60 s) using the $^{28}Si^{2+}$ signal, and measurement by 20 cycles of $^{7}Li^{+}$ (counting time of 5 s) and $^{28}Si^{2+}$ (1 s). The Li concentrations of zircons from modern ocean crust were calculated using the $^{7}Li^{+}/^{28}Si^{2+}$ ratios of sample zircons and that of standard Xinjiang zircon (NMNH #146260, 6.4 ppm Li; Ushikubo et al. 2008). The NIST-612 glass was used as a running standard to monitor analysis conditions. The count rates of $^{7}Li^{+}$ of sample zircons that have low Li concentration (typically <3 ppb) tend to decrease with each consecutive measurement cycle, which is opposite to the tendency of standard Xinjiang zircon and NIST-612 glass. At these very low concentrations (<1–37 ppb), the measured Li concentration is considered a maximum estimate of the sample zircons. As is the case with oxygen isotope measurements, the bottoms of all individual analysis pits were imaged by SEM (all pits were found to be 'regular').

Results

Oxygen isotopes

Normal magmatic zircons

Two hundred twenty-seven oxygen isotope analyses (with regular pits) were made on 197 zircons preserving magmatic textures (e.g., Fig. 2). Rock-averaged $\delta^{18}O$ for zircons from the 43 samples are summarized in Table 1, and all individual analyses are listed in Online Resource 1. Multiple spots were analyzed on selected grains when distinct domains were identified in CL. With the exception of low [Ti] rims that are distinctively luminescent in CL, individual grains are homogeneous in $\delta^{18}O$ within analytical uncertainty. The overall average $\delta^{18}O$ determined for normal magmatic zircons is 5.2 ± 0.5‰. This value is indistinguishable from the value of 5.3 ± 0.8‰ (2SD) reported by Cavosie et al. (2009) for 68 analyses on 24 zircons, which were analyzed in thin sections of ocean-crust gabbro and serpentinite, and can be considered characteristic of zircon formed in MOR settings. The $\delta^{18}O$(Zrc) value of 5.2 ± 0.5‰ is consistent with the primitive value in equilibrium with the mantle at magmatic temperatures (5.3 ± 0.6‰, 2SD), first determined by analysis of zircons from kimberlite by laser fluorination (Valley et al. 1998; Page et al. 2007b).

Figure 4 shows average $\delta^{18}O$ for each crystal of normal magmatic zircon plotted versus host rock, and organized left to right by geographic location (sample numbers are given in Table 1); 3–11 grains were analyzed per rock. Small differences in $\delta^{18}O$(Zrc) are apparent between individual rock-to-rock average values, which vary from 4.9 to 5.6‰, but the average $\delta^{18}O$(Zrc) for different rock types are equivalent (Fig. 5a–d). The $\delta^{18}O$ values recorded by all magmatic ocean-crust zircons are extremely uniform, and the variability of 5.2±0.5‰ is only 0.2‰ (2SD) greater than the analytical reproducibility defined by the standard KIM-5 (5.1 ± 0.3‰, Fig. 5a).

Luminescent CL rims

The $\delta^{18}O$ of luminescent CL rims was measured on 7 zircons (15 spots) from plagiogranite samples U1309D-40 and U1309D-1415 (Table 1). The average $\delta^{18}O$ is 4.8 ± 0.2‰ ($N = 15$), with average values for individual rims varying from 4.6 to 4.9‰ (Fig. 4e). Replicate measurements are reproducible and $\delta^{18}O$ values are consistently 0.3–0.4‰ lower than cores and other magmatic zircons from the same

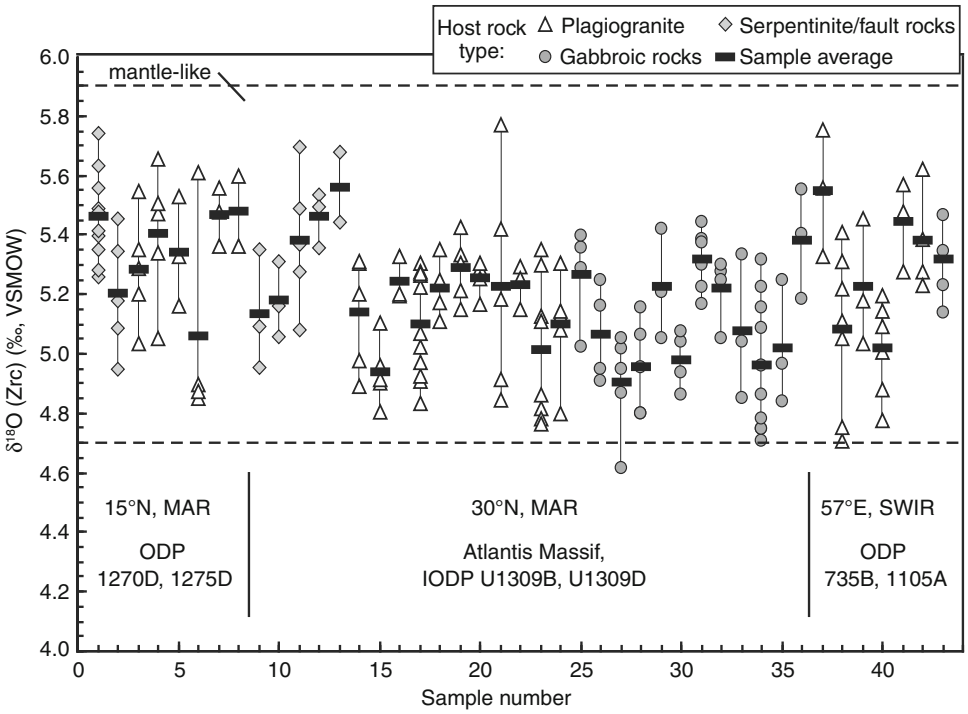

Fig. 4 δ^{18}O(Zrc) of individual magmatic zircons from ocean crust analyzed by ion microprobe. The average is 5.2 ± 0.5‰ (2SD) with an overall range of 1.1‰ for 197 zircons from 43 rocks. Differences within and between individual rock samples are within analytical uncertainty (rock-averaged values shown as a *bold dash*). Each *column* of data points represents zircons from a single rock; sample numbers on the *X* axis are listed in Table 1. The analytical uncertainty (2SD) for individual analyses is ±0.3‰ (2SD). *Dashed horizontal lines* indicate the range for zircon in high-temperature equilibrium with primitive igneous rocks and mantle (5.3 ± 0.6‰, 2SD; Valley et al. 2005)

rock (Fig. 6a, b). These observations indicate that this subtle difference in δ^{18}O is not analytical, but rather a true compositional difference. A Student's *t* test to compare δ^{18}O values for the luminescent rims and normal cores of magmatic grains indicates that they are statistically distinct from one another at >99% confidence. Therefore, these rims are considered separately from the normal magmatic grains without judgment as to genesis. Dark CL rims were also analyzed (Fig. 2), but they did not give consistently higher or lower δ^{18}O values than cores of the same grains.

Porous zircon domains

An additional 56 analyses were performed on domains exhibiting porosity and/or highly perturbed/chaotic CL zoning (Fig. 3a; Table 2). Analysis pits on these domains are very irregular, and contain numerous open cavities. Measured δ^{18}O of the porous domains are highly variable, with values from 0.0 to 5.0‰ (average 3.7 ± 2.6‰, $N = 56$). Porous domains can differ by up to 5‰ from domains in the same grain that preserve normal magmatic textures (e.g., Fig. 3a; Online Resource 1). The low and extremely variable measured δ^{18}O values are consistent with the previous interpretations that the porous domains represent altered zircon, possibly formed by dissolution–re-precipitation reaction of original magmatic zircons in the presence of hydrothermal fluids (Grimes et al. 2009).

Given the highly irregular texture of associated ion microprobe pits and possible analysis of inclusions, data from these pits are less accurate than analyses with regular smooth-bottomed pits. Further investigation with a much smaller beam spot is required to determine whether the measured δ^{18}O values are characteristic of crystalline zircon, rather than zircon + inclusions, or if instrumental bias is variable during secondary-ion extraction from these highly irregular pits. Thus, evaluation of δ^{18}O measured in porous zircon domains is beyond the scope of this study, and these domains are excluded from the following discussion. However, all analyses are reported in Table 2 and Online Resource 1.

Lithium concentration

The Li concentrations measured in 32 ocean-crust zircons hosted by plagiogranite, evolved gabbro, and fault schist are <0.001–0.04 ppm (Table 3). These concentrations are consistent with values previously determined for magmatic zircons from mantle sources, and are lower by factors of 100–10,000 relative to zircons from continental settings (typically 1–100 ppm; Ushikubo et al. 2008; Bouvier et al. 2009).

Discussion

Small variations in δ^{18}O of zircons from ocean crust

Normal magmatic zircon

The in situ ion microprobe data show that magmatic zircons in plutonic crust formed at slow spreading MORs

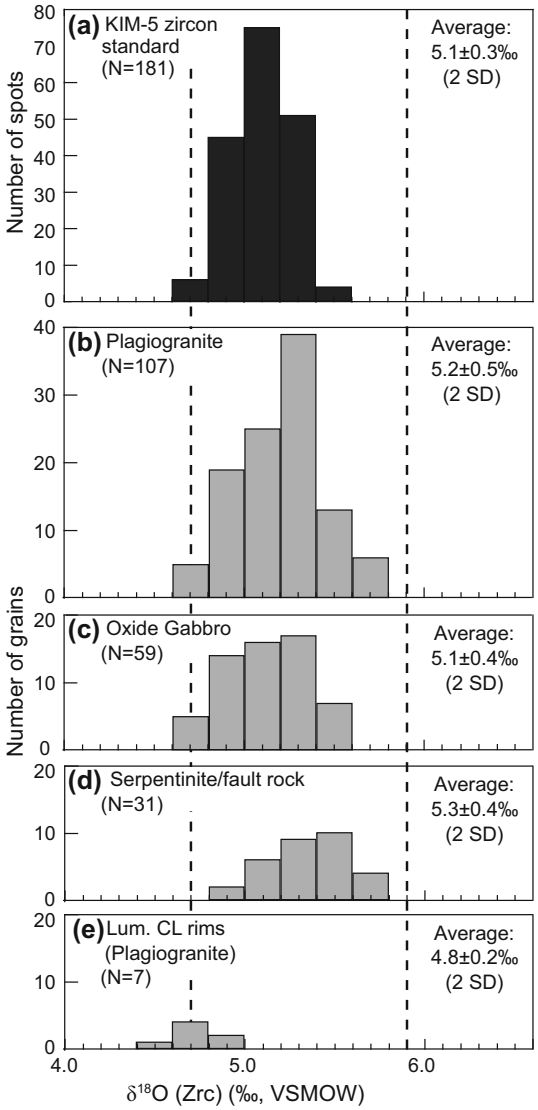

Fig. 5 Histograms of δ^{18}O(Zrc) for **a** all spots analyzed on zircon standard KIM-5 by ion microprobe over three separate sessions, **b–d** single grain-averaged δ^{18}O values of ocean-crust zircons from plagiogranite, evolved gabbro, and fault schist, and **e** luminescent CL rims. *Dashed vertical lines* indicate range of mantle-like values as in Fig. 4 (5.3 ± 0.6‰; Valley et al. 2005)

preserve quite uniform δ^{18}O values that are indistinguishable from values in high temperature equilibrium with a mantle source reservoir. These data indicate that none of the magmas parental to zircon in this study experienced significant contamination of oxygen-isotope ratios by altered crustal material prior to crystallization. A small degree of variability is evident in rock-to-rock average values, which differ by at most 0.7‰ (±0.3, 2SD) (Fig. 4; Table 1), comparable to the range of values defined by zircon megacrysts from kimberlites (Valley et al. 1998; Page et al. 2007b) and for analyses of the homogeneous KIM-5 zircon standard. To evaluate potential contributions to the small variation in rock-averaged values of δ^{18}O(Zrc), we attempt to delimit shifts in δ^{18}O(Zrc) that can arise due to changing crystallization temperature and parental melt composition (see Fig. 7). This is done by calculating the δ^{18}O(Zrc) for representative melt compositions assuming equilibrium between CIPW-normative minerals (Fig. 7a) and zircon over a range of magmatic temperatures. Since Δ^{18}O(mineral–mineral) values increase with falling temperature, the δ^{18}O of constituent minerals will change as temperature drops even if δ^{18}O(WR) is held constant (Fig. 7a; see Eiler 2001; Valley 2003 for additional information). Calculations were made for published whole-rock compositions of plagiogranite from ODP Hole 735B (Niu et al. 2002) with high (70 wt.%), average (62 wt.%) and low (54 wt.%) SiO_2 concentrations (Fig. 7b). The theoretical δ^{18}O(Zrc) in equilibrium with typical MAR N-MORB (~51 wt.% SiO_2; Klein 2003) is also shown for comparison; saturation of zircon within such a melt is not probable, but serves as an example of δ^{18}O(Zrc) behavior in melts with significantly more low-δ^{18}O ferro-magnesian minerals. The δ^{18}O of all normative minerals, zircon, and whole rock are calculated for equilibrium with mantle diopside having δ^{18}O = 5.3‰ at 800°C. Assuming a different initial value for δ^{18}O(cpx) would collectively shift all calculated δ^{18}O values, but it will not change the magnitude of the variation in δ^{18}O(Zrc) over the calculated temperature interval. In other words, the curves in Fig. 7b and c could shift left or right depending on the initial δ^{18}O that is assumed, but the shape of the curves is not changed. Calculated curves for δ^{18}O(Zrc) within each melt composition are shown in Fig. 7b for the temperature interval of 1,000–650°C; however, continuous zircon crystallization from any constant melt composition over such a large interval is unrealistic. Reasonable temperature ranges for zircon crystallization from appropriate melt compositions are shown as heavy bold lines in Fig. 7b and c as a qualitative guide.

Based on the calculated curves in Fig. 7, several interesting observations can be made. First, δ^{18}O(Zrc) is predicted to decrease by at most 0.6‰ from 900 to 650°C in felsic parental magmas (Fig. 7b). This is the approximate range of uncorrected Ti-in-zircon temperatures reported for most terrestrial, crustal zircons (Fu et al. 2008; Grimes et al. 2009). The maximum decrease in δ^{18}O(Zrc) is less (~0.3‰) for intermediate or mafic magmas. The variation in δ^{18}O(Zrc) expected for a single rock would also be smaller, considering typical ranges in Ti-in-zircon crystallization temperatures of ~50–150°C for suites of zircons from single rocks (e.g., Grimes et al. 2009). In a study of different eruptions from the Bishop Tuff magma chamber, Bindeman and Valley (2002) found that δ^{18}O(Zrc) was about ~0.3‰ higher in siliceous melts quenched at 820 vs. 720°C (temperatures determined from oxygen-isotope thermometry on quartz–magnetite pairs).

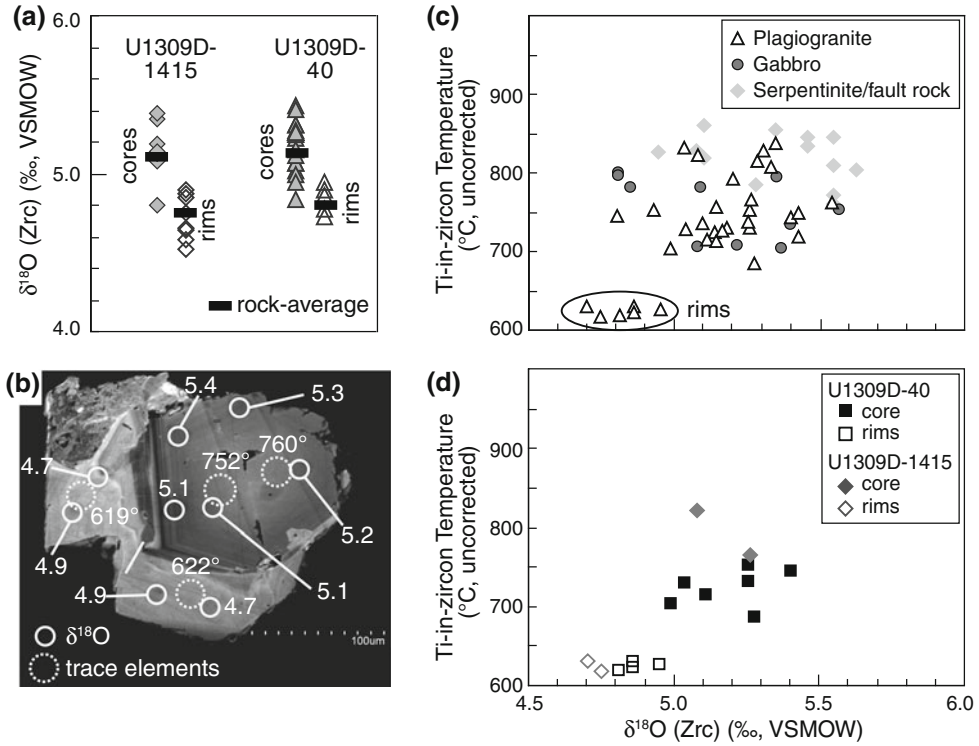

Fig. 6 Comparison of $\delta^{18}O$ with apparent Ti-in-zircon temperature for normal magmatic zircons and late (luminescent in CL) rims. **a** $\delta^{18}O$ for rims (15 spots, 7 rims) and normal magmatic zircons from plagiogranite rock samples U1309D-1415 and U1309D-40. Each data point represents an individual spot analysis. **b** Representative CL image of a single zircon (grain U1309D-40-13) with an oscillatory-zoned core rimmed by a luminescent rim overgrowth; analysis spot locations are shown for $\delta^{18}O$ and Ti-in-zircon temperatures (uncorrected calibration of Ferry and Watson 2007; [Ti] reported by Grimes et al. 2009). Corresponding $\delta^{18}O$(Zrc) versus apparent Ti-in-zircon temperature (uncorrected) measured within the same CL domain are given for **c** all magmatic ocean-crust zircons and luminescent CL rims, and **d** rock samples U1309D-1415 and U1309D-40 only

Table 2 Summary of $\delta^{18}O$ measured by ion microprobe in porous ocean-crust zircons

Number	Location/sample (cruise or Leg/Exp-Site-Hole-core, top)	Depth (mbsf)	Rock type	$\delta^{18}O$ (‰, SMOW)				
				Ave[a]	2SD	Max	Min	Number of analyses
30°N, MAR								
Atlantis Massif (southern wall)								
9	MARVEL2000, *Alvin* 3652-1333	0	Fs(OxGb?)	4.6	0.3	4.7	4.5	2
U1309B average (Plgt)								
15	304-U1309B-7R-1, 77 cm	39	Plgt	4.8	0.5	5.0	4.5	4
U1309D average (Plgt)								
17	304-U1309D-5R-3, 136 cm	40	Plgt	4.7	0.4			1
19	304-U1309D-40R-1, 21 cm	215	Plgt	4.3	0.3	4.4	4.2	2
24	305-U1309D-295R-3, 100 cm	1,415	Plgt	4.1	1.3	5.0	2.4	16
U1309D average (OxGb)								
30	305-U1309D-126R-2, 27 cm	623	OxGb	4.4	0.6	4.7	4.0	4
31	305-U1309D-131R-2, 0 cm	647	OxGb	2.7	3.1	4.9	0.0	20
33	305-U1309D-189R-4, 41 cm	923	OxGb	3.9	1.5	4.4	3.1	3
34	305-U1309D-244R-2, 100 cm	1,175	OxGb	4.5	0.7	4.9	4.0	4

Post SIMS imaging reveals these analysis spots have irregular pit structures, and are therefore considered less precise

[a] Duplicate measurements on single grains can be variable, and so rock-averaged values are calculated using all spot analyses. These data are considered less accurate than regular spots reported in Table 1, based on the irregular ion microprobe pit structure and presence of pores (e.g., Fig. 3)

Table 3 Lithium concentration in magmatic ocean-crust zircons from the Mid-Atlantic Ridge (MAR) measured by ion microprobe

Number[a]	Sample_grain.spot	Rock type[a]	Li (ppm)[b]
ODP Hole 1270D, 14° 45′ N, MAR			
1	1270D-19_8.1	V/D	0.028
1	1270D-19_3B.1	V/D	<0.001
2	1270D-25_6.1	V/D	<0.001
Surface of Atlantis Massif, 30°N, MAR			
9	3652-1333_2.1	FS	<0.004
9	3652-1333_4.1	FS	<0.001
9	3652-1333_5.1	FS	<0.002
9	3652-1333_6.1	FS	<0.002
9	3652-1333_7.1	FS	<0.001
10	3646-1205_6.1	FS	<0.001
10	3646-1205_3.1	FS	<0.003
IODP Hole U1309D, 30° N, MAR			
17	U1309D-40_9.1	Plgt	<0.002
17	U1309D-40_9.2	Plgt	<0.002
17	U1309D-40_13.1	Plgt	<0.001
17	U1309D-40_14.1	Plgt	<0.002
19	U1309D-215_4.1	Plgt	0.037
19	U1309D-215_4.2	Plgt	<0.001
19	U1309D-215_9.1	Plgt	0.014
19	U1309D-215_11.1	Plgt	0.008
29	U1309D-564_2.1	OxGb	<0.002
29	U1309D-564_5.1	OxGb	<0.001
21	U1309D-570_1.1	Plgt	<0.002
21	U1309D-570_2.1	Plgt	<0.001
21	U1309D-570_3.1	Plgt	<0.003
–	U1309D-588_3.1	Gb	0.008
–	U1309D-588_5.1	Gb	0.017
–	U1309D-588_6.1	Gb	0.003
31	U1309D-647_4.1	OxGb	0.017
31	U1309D-647_9.1	OxGb	0.009
31	U1309D-647_10.1	OxGb	0.010
24	U1309D-1415_5.2	Plgt	0.002
24	U1309D-1415_6.1	Plgt	<0.001
24	U1309D-1415_7.1	Plgt	<0.002
24	U1309D-1415_7B.1	Plgt	<0.001

[a] Rock-sample number same as in Table 1

[b] Values preceeded by '<' are an upper limit

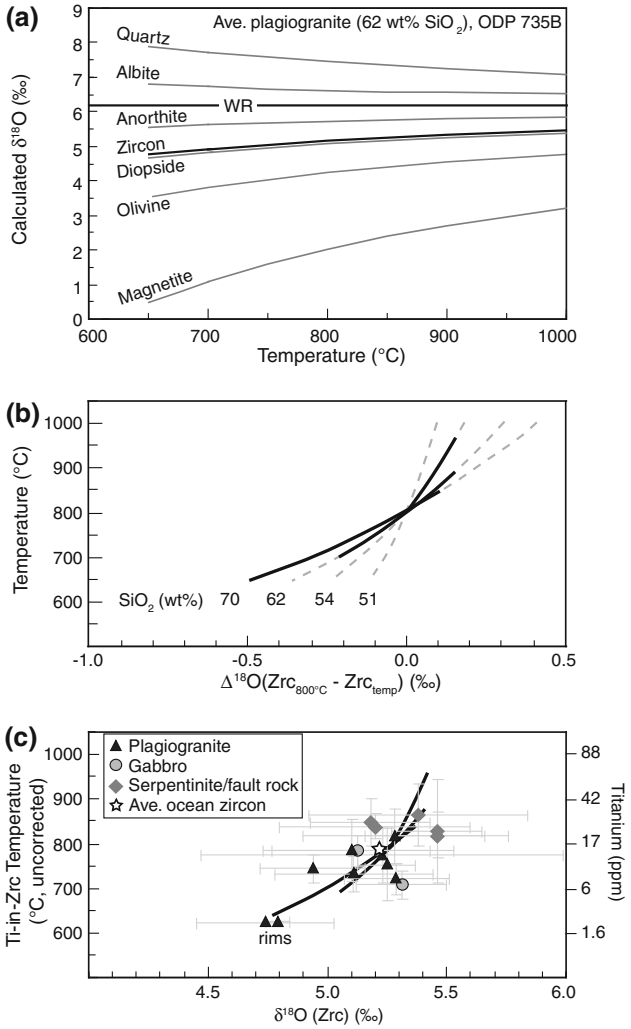

Fig. 7 Calculated δ^{18}O(Zrc) for variable crystallization temperature and parent melt composition. **a** δ^{18}O values of CIPW-normative minerals, zircon, and whole rock calculated for average oceanic plagiogranite from ODP Hole 735B, SWIR (~62 wt% SiO_2; Niu et al. 2002), assuming equilibrium with MORB (fractionation factors from Valley 2003). **b** Calculated curves showing the maximum shift in δ^{18}O for zircons crystallized over the temperatures range 1,000 to 650°C from melts with various SiO_2 concentrations. *Solid lines* represent reasonable temperature ranges for zircon crystallization from the respective melt compositions. Scale on the *X* axis reflects the shift in δ^{18}O relative to a hypothetical zircon crystallized at 800°C. **c** Rock-averaged δ^{18}O(Zrc) versus Ti-in-zircon temperatures (*error bars* represent 2SD). Ti-in-zircon temperatures (uncorrected calibration of Ferry and Watson 2007) are reported in Table 1 and were calculated from [Ti] data reported by Grimes et al. (2009). *Solid black curves* are the same as in **b**, and are positioned assuming equilibrium with $\delta^{18}O_{diopside} = 5.3‰$ at 800°C. Average ocean-crust zircon is shown (800°C, $\delta^{18}O = 5.2$)

These observations are in agreement with our calculations for melts with ~70 wt.% SiO_2. A second observation from these calculations is that larger shifts in δ^{18}O(Zrc) and increased Δ^{18}O(WR-Zrc) occur with increasing SiO_2 concentration of the parental melt. This is because a greater abundance of high δ^{18}O phases (quartz and feldspar) causes lower δ^{18}O phases (including zircon) to be shifted down by a greater amount with decreasing temperature to achieve ^{18}O mass balance. During closed system differentiation by fractional crystallization, δ^{18}O(magma) reportedly can increase by 1–1.5‰ from mafic to felsic compositions (e.g., Muehlenbachs and Byerly 1982; Taylor and Sheppard 1986). However, because the changing chemistry of the melt causes Δ^{18}O(magma-zircon) to

increase along with the δ^{18}O(magma), the magnitude of change in δ^{18}O(Zrc) will be significantly less (Fig. 7; Valley et al. 1994; Valley 2003; Lackey et al. 2008). This conclusion highlights the important fact that magma-differentiation processes producing changes in δ^{18}O(WR) do not necessarily produce equivalent shifts in constituent minerals.

Finally, from the calculated curves in Fig. 7, it is apparent that δ^{18}O values outside of the expected mantle-like range of 5.3 ± 0.6‰ present strong evidence for interactions with non-mantle-δ^{18}O components. Rock-averaged δ^{18}O(Zrc) and Ti-in-zircon temperatures are shown in Fig. 7c along with curves from Fig. 7b. Making the assumption of equilibrium between the zircon-producing magmas and mantle diopside with δ^{18}O ~5.3‰ (comparable to ODP Hole 735B olivine gabbros; Gao et al. 2006) at 800°C, the calculated curves completely overlap the measured data within analytical uncertainties. The analytical uncertainties associated with measured δ^{18}O and Ti and/or accuracy of the Ti-in-zircon thermometer (e.g., Watson and Harrison 2005; Ferry and Watson 2007; Fu et al. 2008; Hofmann et al. 2009) are significant relative to the narrow range of values observed for δ^{18}O(Zrc) and may obscure correlations with temperature when comparing single grains (Fig. 6c) or rock-averaged values (Fig. 7c). Corrections of ±50°C to the zircon crystallization temperature relative to the uncorrected temperatures will not significantly degrade the overlap with the calculated curves.

Overall, the calculations indicate that small differences in δ^{18}O(Zrc) values of up to a few tenths of permil could be caused by variations in crystallization temperature and parent melt compositions. The variation in δ^{18}O(Zrc) defined by igneous ocean-crust zircons (±0.5‰, 2 SD) is remarkably narrow and mantle-like, and only slightly larger than reproducibility of the standard zircon KIM-5 (±0.3‰, 2SD) (Fig. 5). Thus, the variability among zircons from different samples (Fig. 4) can be fully explained by analytical precision, with possibly a small temperature effect.

Low δ^{18}O luminescent CL rims

Most single zircons, as well as suites of zircon from individual rocks, record uniform δ^{18}O values that overlap within analytical uncertainty. Thus, crystallization over a narrow temperature interval is implied. However, both the measured δ^{18}O and [Ti] of luminescent rims are distinctive from normal magmatic zircon cores (Fig. 6). These rims record Ti-in-zircon temperatures that are 100–160°C lower than cores and other normal magmatic grains from the same rocks (786–730 vs. 625°C, uncorrected; Fig. 6; Table 1), and δ^{18}O(Zrc) values that are 0.3–0.4‰ lower than cores and normal magmatic grains from the same rock (Table 1). The decreases in δ^{18}O(Zrc) and Ti-in-zircon temperature agree extremely well with predicted trends (Fig. 7c) for average to high SiO_2 plagiogranite. Thus, even these relatively low δ^{18}O values recorded by the rims can be explained by crystallization from a melt preserving δ^{18}O inherited from equilibrium with the mantle. Furthermore, the δ^{18}O values support the growth of these rims at lower temperatures as indicated by Ti-in-zircon thermometry.

Primary magmatic δ^{18}O values of crust-forming magmas at slow-spreading MORs

Unaltered primitive ocean gabbros are expected to have whole-rock δ^{18}O values similar to fresh MORB (~5.6 ± 0.2‰; Eiler 2001). In contrast, measured δ^{18}O(WR) values for gabbros from many of the crustal sections sampled for zircon are widely variable, with values ranging from 1.4 to 10.2‰ (Fig. 8; Stakes et al. 1991; Alt and Bach 2006; Alt et al. 2007; McCaig et al. 2010). This range of δ^{18}O(WR) values reflects extensive subsolidus hydrothermal alteration by seawater-derived fluids with variably shifted compositions over a range of temperatures and water–rock ratios. In contrast, oxygen-isotope ratios of constituent minerals within gabbros from the lower 1 km of ODP Hole 735B measured by UV laser fluorination were found to be more uniform and mantle-like (Gao et al. 2006; reproduced in Fig. 8c). Rock-averaged δ^{18}O values reported for olivine range from 4.5 to 5.8‰ with all, but two samples averaging 5.0–5.1‰, while clinopyroxenes from the same samples range from 5.1 to 5.6‰. The uniform, mantle-like δ^{18}O values for fresh olivine limit variations in δ^{18}O of primitive MORB parent magmas that constructed this multiply intruded crustal section.

In contrast to the primitive olivine-bearing gabbros, the δ^{18}O(WR) values of late-stage melts that produced Fe-enriched gabbros and plagiogranites remain poorly constrained. The magmatic δ^{18}O(WR) of these rock types could differ from fresh MORB due to greater normative abundances of low δ^{18}O minerals (magnetite and ilmenite) in the evolved oxide gabbros and high δ^{18}O minerals (quartz and feldspar) in plagiogranite. Furthermore, magmatic δ^{18}O would be expected to reflect any contamination of the magmas. Measured δ^{18}O(WR) values for oxide gabbros from ODP Hole 735B show considerable variation from 3.9 to 7.2‰ (Alt and Bach 2006). A similar range (4.6–7.6‰) is reported from four plagiogranite samples (WR) from the same drill core (Kempton et al. 1991; Alt and Bach 2006). The ~3‰ variation in δ^{18}O for both rock types is in stark contrast to the narrow range of δ^{18}O values recorded by ocean-crust zircons (Fig. 8). The δ^{18}O(WR) and δ^{18}O(Zrc) values can be compared through an

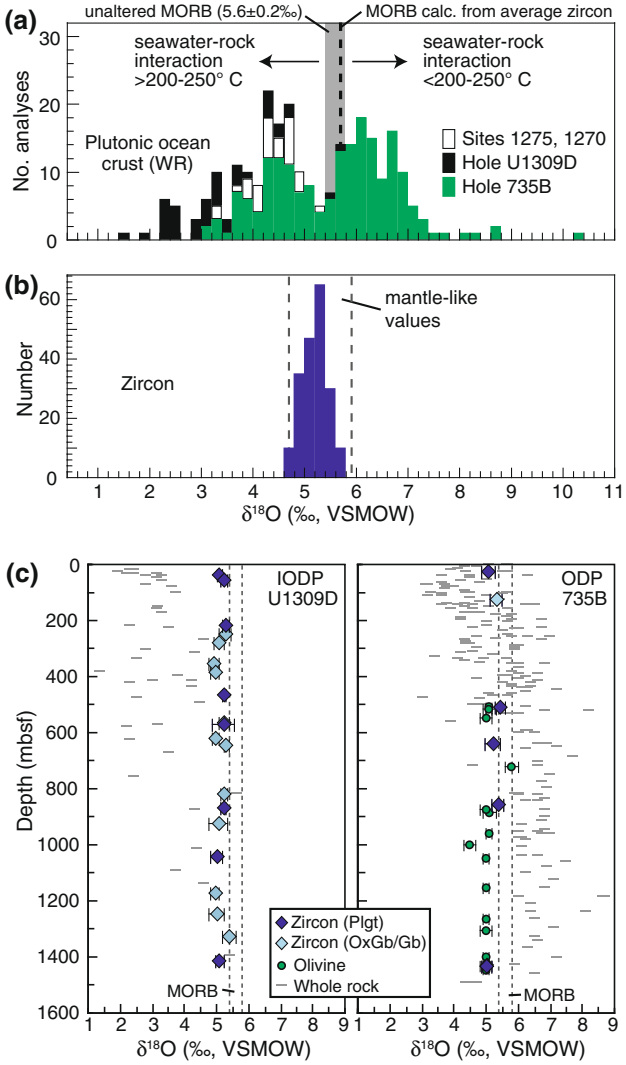

Fig. 8 **a** Whole rock (WR) $\delta^{18}O$ measured in crustal sections sampled for zircons in this study (Fig. 1). The average value for unaltered MORB is *labeled*, and shown as a *shaded* vertical field ($\delta^{18}O = 5.6 \pm 0.2‰$; Eiler 2001). The *dashed vertical black line* represents $\delta^{18}O$ calculated for a magma with 50 wt% SiO_2 (~MORB) in equilibrium with the average $\delta^{18}O$(Zrc) hosted by gabbro (5.1‰, this study; $\Delta^{18}O$(WR-Zrc) from Lackey et al. 2008). **b** $\delta^{18}O$ of magmatic ocean-crust zircons analyzed in this study. *Dashed lines* delimit the range of $\delta^{18}O$(Zrc) in equilibrium with the mantle at magmatic temperatures (5.3 ± 0.6‰; e.g., Valley et al. 2005). **c** Plots of $\delta^{18}O$ versus sampling depth below the seafloor for whole rocks (McCaig et al. 2010) and zircons in IODP Hole 1309D (this study), and whole rock (Alt and Bach 2006), olivine (laser fluorination; Gao et al. 2006), and zircon in ODP Hole 735B. Zircon data represent average values for each rock; *error bars* shown at 2SE (standard error; Table 1). The *vertical dashed lines* indicate $\delta^{18}O$ for unaltered MORB

empirical relation developed by Lackey et al. (2008) that provides a method for estimating magmatic $\delta^{18}O$(WR) values from measured $\delta^{18}O$(Zrc) and SiO_2(WR) concentration:

$$\begin{aligned}\Delta^{18}O(\text{magma-zircon}) &= \delta^{18}O(\text{magma}) - \delta^{18}O(\text{Zrc}) \\ &\approx 0.0612(\text{wt\% SiO}_2\text{ magma or whole rock}) - 2.50‰.\end{aligned} \quad (1)$$

Using Eq. 1, primary magmatic $\delta^{18}O$(WR) values can be estimated, providing a framework for interpreting measured $\delta^{18}O$(WR). Oxide gabbro from Holes 735B and U1309D contain ~45–50 wt% SiO_2 (Dick et al. 2000; Blackman et al. 2006; Godard et al. 2009), and taken with the average $\delta^{18}O = 5.1‰$ for zircons from oxide gabbro (Table 1) results in calculated $\delta^{18}O$(WR) of 5.4–5.7‰. These values are similar to, or slightly below, the values for typical MORB, which is consistent with the accumulation of low $\delta^{18}O$ ferro-magnesian minerals and Fe–Ti oxides. The SiO_2 concentration of plagiogranite from in situ ocean-crust varies from ~54 to 75 wt.% (Niu et al. 2002; Kelemen et al. 2004; Blackman et al. 2006; Godard et al. 2009). When considering the average plagiogranite $\delta^{18}O$(Zrc) of ~5.2‰, calculated $\delta^{18}O$(WR) would be 6.0–7.3‰. The narrow range of calculated $\delta^{18}O$(WR) indicates that variable measured $\delta^{18}O$(WR) reflects significant subsolidus exchange between hydrothermal fluids with some minerals of the rock.

The $\delta^{18}O$ measured in ocean-crust zircons suggests that, similar to primitive magmas that crystallized the olivine-bearing gabbros in Hole 735B, the most evolved magmas sampled along the MAR and SWIR retained mantle-like oxygen-isotope ratios at the time of zircon crystallization. The fractionation of oxygen isotopes between zircon and olivine in Hole 735B is also consistent with this interpretation, giving $\Delta^{18}O$(Zrc-olivine) = ~0.2‰ in agreement with the previously observed fractionation between these minerals for high-temperature equilibrium with the mantle (e.g., Valley 2003; Cavosie et al. 2009).

Timing and extent of hydrothermal alteration relative to plagiogranite formation beneath slow spreading MORs

The formation of plagiogranites has been ascribed to a variety of processes including 85–90% fractional crystallization of MORB, liquid immiscibility with Fe-enriched melts, and hydrous partial melting of gabbro at temperatures of 900–1,000°C (review by Koepke et al. 2007). All of these hypotheses have been proposed for plagiogranites sampled from ODP Hole 735B (Natland et al. 1991; Dick et al. 2000; Natland 2002; Niu et al. 2002; Koepke et al. 2004). Most recently, experimental studies have shown that hydrous partial melting of primitive ocean gabbros can occur if temperatures exceed 900°C at 200 MPa and at high water activities (Koepke et al. 2004). Geochemical

similarities between natural plagiogranites and experimental melts led Koepke et al. (2007) to conclude that hydrous partial melting is much more common than previously thought. In particular, the TiO_2 concentrations of most plagiogranites overlap with experimental melts formed by hydrous partial melting of typical gabbros above 900°C and 200 MPa, but are largely distinct from melts expected from fractional crystallization of MORB. Amphibole–plagioclase pairs suggesting temperatures up to ~900°C have been reported in oceanic gabbros from the MAR and SWIR, and are cited as evidence for the presence of water at temperatures sufficient for partial melting to occur (e.g., Bosch et al. 2004; Koepke et al. 2007). In slow spreading ocean crust, it is proposed that seawater-derived fluids penetrate the lower crust along deep-rooting axial fault systems and trigger melting (Koepke et al. 2007; Jöns et al. 2009).

The process of hydrous partial melting triggered by seawater-derived fluids is neither supported nor rejected based on the measured oxygen-isotope ratios in zircon because very small amounts of water are sufficient to flux melting. However, the $\delta^{18}O$(Zrc) data can be used to evaluate the extent of fluid–rock interaction prior to melting that may have occurred to form plagiogranite magmas. The volume of water necessary to trigger hydrous partial melting determined experimentally at ~1–2 kbars is small, and ~1 wt.% H_2O (relative to the total mass of rock) may be sufficient to produce ~10 wt.% of a felsic, water-saturated melt (Koepke et al. 2007). This is equivalent to a water–rock ratio (W/R) of 0.02 (atoms of oxygen), assuming that the oxygen in water exchanges with the entire volume of the protolith. In the absence of recrystallization, exchange with unmelted rock could only progress by diffusion. Temperatures <1,000°C are below the blocking temperature for diffusion of oxygen in 1 mm and larger crystals of pyroxene for time scales relevant to MOR magmatism based on hydrous experiments (Farver 1989; see Valley 2001). Therefore, diffusion of oxygen during fluid–rock interactions below ~1,000°C would be limited predominantly to plagioclase, which has much faster diffusion rates for oxygen and responds relatively rapidly to hydrothermal alteration. For a typical gabbro with ~50% plagioclase, it is a reasonable assumption that only half the total rock volume would exchange oxygen, thus increasing the W/R ratio for the portion of gabbro open to exchange by a factor of two. At high temperatures >600°C and assuming seawater ($\delta^{18}O = 0‰$) as the hydrating fluid, W/R = 0.04 would shift $\delta^{18}O$(magma) by ~−0.3‰ upon melting. The shift in $\delta^{18}O$ would be smaller if hydrothermal fluids with $\delta^{18}O > 0‰$ were involved. Changes in $\delta^{18}O$ of <0.3‰ relative to mantle-like values would be comparable to the analytical uncertainties of the present study, and would be difficult to resolve. Alternatively, infiltrating water-rich fluid could exchange with only the portion of rock that ultimately undergoes melting. This model would be reasonable if hydration and subsequent melting were rapid and concentrated along grain boundaries. In this case, W/R ratios would be ~0.2 for the melt (assuming 10% melting of the protolith by 1 wt.% water), shifting $\delta^{18}O$(magma) by −1‰ at temperatures >600°C and assuming seawater as the hydrating fluid. Changes in this magnitude would be readily observable in $\delta^{18}O$(Zrc) values.

From the present study, $\delta^{18}O$ of magmatic zircons provide no evidence for interactions between low (or high) $\delta^{18}O$ fluids and gabbro at high temperatures prior to or synchronous with melting. We caution that very small degrees of water–rock interaction would likely not be discernable using $\delta^{18}O$(Zrc). However, any model for formation of plagiogranite at slow spreading MOR involving partial melting of a hydrated gabbro requires that hydration/alteration did not change $\delta^{18}O$ of the protolith or resultant partial melt by more than a few tenths of a permil relative to mantle-like values. Greater extents of seawater contamination may occur beneath fast-spreading ridges, where chlorine excesses in lavas indicate assimilation involving seawater-altered rocks (e.g., Michael and Cornell 1998), and could possibly produce resolvable shifts in $\delta^{18}O$(Zrc).

Although the infiltration of seawater into gabbroic ocean crust is well documented, the timing with regard to the formation of the latest-stage magmas was previously not clear. In slow-spreading ridge environments, incipient infiltration of seawater deep in the crust may occur during plate spreading and development of deep-rooting fault systems. The flux of seawater is greatest at shallow levels, at lower temperature, and in association with the development of brittle crack networks (e.g., Lister 1974; Gregory and Taylor 1981; Mével and Cannat 1991; Stakes et al. 1991). As a result of interactions with seawater, gabbros from drill holes on the MAR and SWIR recovered near the seafloor/detachment fault scarp exhibit shifts in $\delta^{18}O$(WR) values to 2–3‰ (Fig. 8), reflecting significant hydrothermal alteration above 200–250°C. Studies of the mineralogy, fluid inclusions, and isotopic signatures of plastically deformed gabbros in the upper 500 m of ODP Hole 735B led Stakes et al. (1991) and Vanko and Stakes (1991) to infer incipient seawater migration began at temperatures >700°C. Based on the trace element and isotopic studies of gabbros in ODP Hole 735B, Hart et al. (1999) offered a model where incipient seawater circulation contributed to the generation and mobilization of evolved, hydrous melts prior to complete solidification of the cumulate pile. From isotopic studies of hydrous

dioritic/gabbroic dikes in the lower crust of the Oman ophiolite, extensive interactions between seawater and hydrous late-stage magmas (water/rock ratios >1) have been inferred on the basis of strontium- and oxygen-isotope ratios measured in high-temperature amphibole and clinopyroxene (Bosch et al. 2004). These hydrous magmatic dikes are interpreted as the discharge conduits for a seawater hydrothermal circulation system acting at temperatures up to 1,000°C (Nicolas et al. 2003; Bosch et al. 2004; Nicolas and Mainprice 2005). From magmatic δ^{18}O recorded by zircon in this study, we find no evidence for such extensive water–rock interactions prior to the formation of late-stage plagiogranite magmas. If melting of gabbros is a common mechanism by which plagiogranites in slow-spreading ocean crust form, the melting must typically occur prior to the extensive water/rock interaction that significantly altered δ^{18}O(WR) in many rocks. These results support conclusions that extensive seawater–rock interaction post-dates the last stages of magmatic crystallization (e.g., Gregory and Criss 1986; Stakes et al. 1991; Coogan et al. 2001), and thus follows complete solidification of the gabbroic ocean crust.

As an alternative to melting fluxed by seawater-derived fluids, perhaps magmatic fluids contribute to hydration and partial melting of gabbros to form plagiogranite melts. Again, the total amount of fluid necessary is not large relative to volumes of mafic magma. Saturation and exsolution of fluids from MORB could occur after ~90% fractional crystallization (Nehlig 1993; Dixon et al. 1995). Hydrogen isotopes and fluid inclusion studies on ocean gabbros from ODP Hole 735B provide evidence for a hydrothermal system that evolved from dominantly magmatic to heated seawater and finally to late cold seawater (Vanko and Stakes 1991; Kelley 1996; Kelley and Früh-Green 1999; Bach et al. 2001). Maeda et al. (2002) argued that microscopic veins cutting olivine gabbro in Hole 735B formed from high-temperature, hydrous alteration up to 1,000°C. These veins, comprising clinopyroxene, orthopyroxene, brown amphibole, and plagioclase, were interpreted as the reaction products with magmatic fluids based on the textural evidence that they preceded any deformation (ductile or brittle), which is required for the transport of seawater into the lower crust. If partial melting of gabbros was triggered by deuteric fluids, the resulting δ^{18}O(WR) of the solidified melts would not differ significantly from unaltered ocean crust, and resulting δ^{18}O(Zrc) would be ~5.2‰. Because oxygen-isotope ratios would not be affected, other means must be found to test this hypothesis. Perhaps, the halogen compositions of high-temperature amphibole, D/H of melt inclusions, or chlorine isotopic signatures can provide further insight into the origin of fluids during incipient hydrothermal alteration of lower crustal gabbros.

Zircons in serpentinites and fault rocks

Zircons from several highly deformed and completely recrystallized fault rocks sampled from oceanic detachment systems were also analyzed. The seafloor at these sampling locations coincides with large-offset normal fault scarps (e.g., Blackman et al. 2004; Schroeder et al. 2007) that facilitated significant flow of seawater-derived fluids based on whole-rock strontium and oxygen isotopes (Alt et al. 2007; Delacour et al. 2008; Jöns et al. 2009). As with other samples in this study, zircons hosted in cm scale greenschist-grade shear zones (dominantly chlorite + actinolite/tremolite) collected in Hole 1270D preserve normal mantle-like δ^{18}O (rock-averaged δ^{18}O(Zrc) values of 5.2 ± 0.4‰ and 5.5 ± 0.3‰) (Table 1). Zircons in metasomatized fault schists recovered at 30°N on the southern wall of Atlantis Massif also preserve mantle-like δ^{18}O (5.2–5.6 ± 0.3‰) (Table 1). Along with the CL zoning, REE patterns, and chemical characteristics (Grimes et al. 2009), these oxygen-isotopic constraints indicate an igneous origin the zircon from melts in equilibrium with the mantle. Thus, despite extensive hydrothermal alteration of the host rocks, there is no evidence that the zircons were either precipitated from, or altered by, hydrothermal fluids. The zircons likely originated in evolved melts emplaced prior to deformation, or from syn-kinematic magmas injected into the active fault zone that perhaps formed by partial melting triggered by ingress of seawater (e.g., Jöns et al. 2009). In either case, the uniform mantle-like δ^{18}O(Zrc) values indicate that these evolved melts were generated and zircon crystallized prior to migration of large volumes of seawater-derived fluids and alteration of the wall rocks along these fault zones.

Are oceanic plagiogranites the source of >3.9 Ga detrital zircons from the early crust?

Many authors have discussed a possible granitic source in continental or proto-continental crust for the 4.4–3.9 Ga detrital zircons from the Jack Hills, Western Australia, based on mineral inclusions, REE and Ti geochemistry, and isotopic characteristics (see reviews in Cavosie et al. 2007; Trail et al. 2007; Ushikubo et al. 2008; Harrison 2009). Oxygen-isotope ratios that are mildly elevated relative to mantle zircons suggest the source magmas incorporated supracrustal material that had interacted with surface water at low temperatures, and that liquid oceans existed by 4.3 Ga (Valley et al. 2002). Harrison (2009) further suggests a fully developed continental crust with true granites and plate tectonics by 4.4 Ga.

An alternative hypothesis suggests formation of Jack Hills zircons in magmas analogous to those found in modern ocean crust (e.g., Coogan and Hinton 2006) and

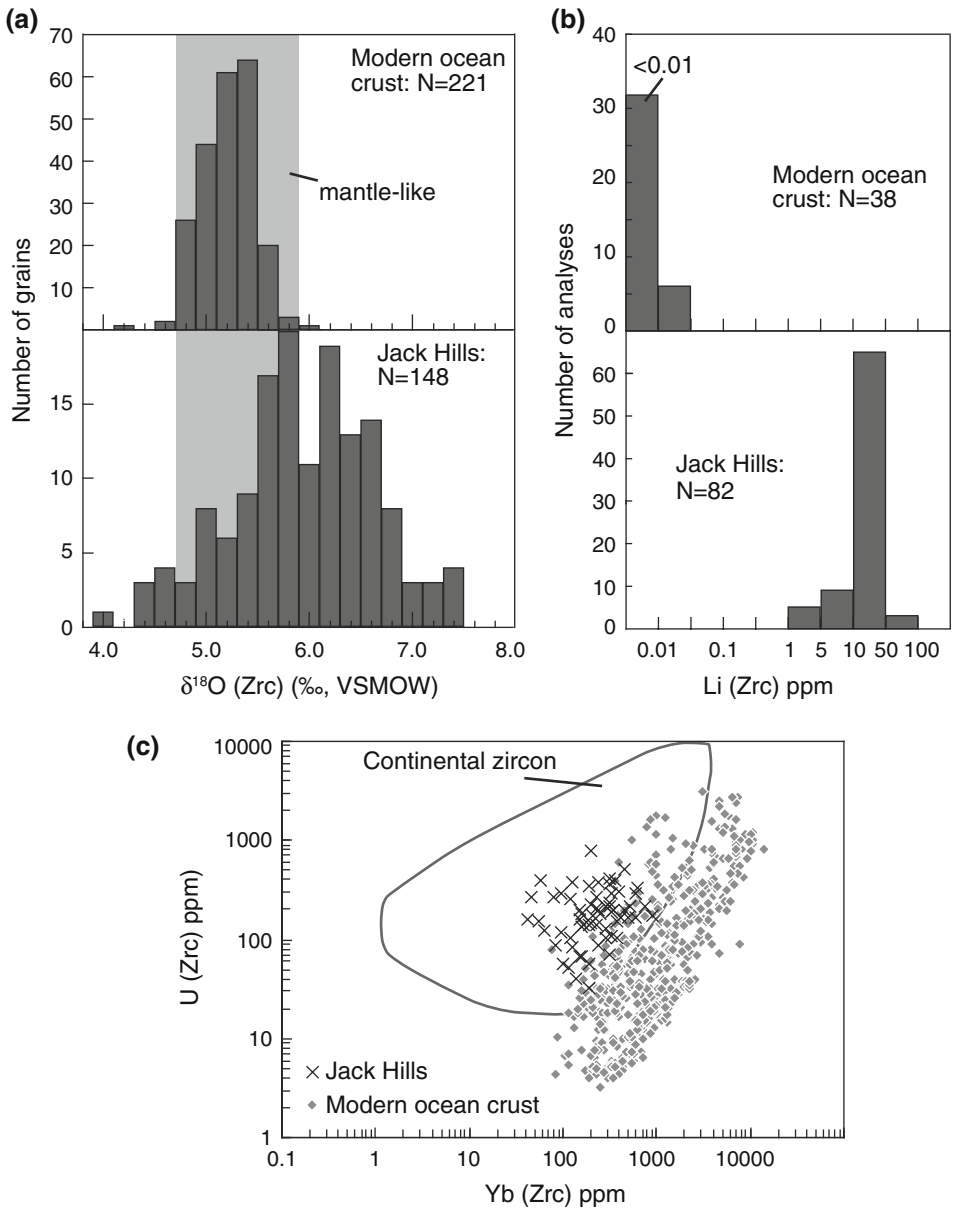

Fig. 9 Comparison of trace element and oxygen isotope geochemistry of ocean-crust zircons and >3.9 Ga detrital zircons from the Jack Hills, Australia. **a** Histograms showing δ^{18}O(Zrc) for average values of individual zircon grains. Ocean crust zircon data are for magmatic zircons from plagiogranite, gabbro, and meta-ultramafic host rocks sampled along the Mid-Atlantic and Southwest Indian Ridges (this study; Cavosie et al. 2009). Jack Hills zircons include data reviewed by Cavosie et al. (2007), Trail et al. (2007), and Harrison et al. (2008), and include grain-averaged values from spots on domains with Pb/U age concordance of >85% (see Cavosie et al. 2007). **b** Lithium concentration in magmatic zircons (this study; Ushikubo et al. 2008). **c** Discrimination diagrams based on U and Yb (modern values). Ocean-crust zircon data and the field for continentally derived magmatic zircons are from Grimes et al. (2009); >3.9 Ga Jack Hills zircon data are from Maas et al. (1992), Crowley et al. (2005), and Cavosie et al. (2006). Multiple analyses from the same grain were averaged prior to plotting

ophiolites formed at a MOR (Rollinson 2008). Coogan and Hinton (2006) asserted that Hadean detrital zircons are not chemically distinct from ocean-crust zircons. Rollinson (2008) showed that plagiogranite-hosted zircons from the Oman ophiolite have Th/U ratios that largely overlap with Jack Hills zircons, and speculated that the pre-3.9 Ga zircons could have elevated δ^{18}O if they crystallized from plagiogranite magmas formed by melting of mafic crust that had been altered by seawater at temperatures <200–250°C. These studies argue that the pre-3.9 Ga zircons came from mafic crust and do not support the existence of granitic rocks or continental crust.

Cooling of ocean crust to temperatures below 250°C and subsequent remelting as proposed by Rollinson (2008) to elevate δ^{18}O(magma) and δ^{18}O(Zrc) values requires migration off-axis away from the active zone of magma intrusion. The subsequent reheating necessary to trigger partial melting of high-δ^{18}O rocks would be difficult energetically because of the off-axis location. Melting of low-δ^{18}O rocks altered early by high-temperature hydrothermal fluids while still near the ridge axis seems more probable, but would produce magmas with relatively low δ^{18}O and thus distinct from the mildly elevated δ^{18}O(Zrc) values reported in many pre-3.9 Ga Jack Hills zircons.

Furthermore, three lines of geochemical evidence clearly distinguish ocean-crust zircons from Jack Hills detrital zircons (Fig. 9) demonstrating that oceanic plagiogranite and evolved gabbro formed at a MOR are not viable analogs to magmas parental to 4.4–3.9 Ga detrital grains. First, zircons from plagiogranite and evolved

gabbro formed at slow spreading MORs consistently preserve mantle-like $\delta^{18}O$ (Cavosie et al. 2009, this study). No zircons with mildly elevated $\delta^{18}O$ values >6.0 have been found in ocean crust. This is in contrast to the Jack Hills zircons with ages >3.9 Ga, many of which record $\delta^{18}O$ from 6.0 to 7.5‰ (Fig. 9a; Cavosie et al. 2007; Harrison et al. 2008). Second, concentrations of Li in normal magmatic ocean-crust zircons (typically <0.04 ppm, Table 3) are several orders of magnitude lower than in Jack Hills zircons (10–60 ppm; Ushikubo et al. 2008) (Fig. 9b). Finally, Grimes et al. (2007) demonstrated using primarily U versus Yb, and U/Yb and Th/Yb ratios that the Jack Hills zircon suite is distinct from ocean-crust zircons formed at both fast and slow spreading MORs (Fig. 9c). Instead, U/Yb ratios of the Jack Hills zircons resemble U/Yb in zircons from Phanerozoic and Archean age continental and island arc crust. Based on the existing geochemical data from ocean-crust zircons, neither plagiogranite- nor evolved gabbro-producing magmas formed in MOR-like environments are viable analogs for the source of the Jack Hills zircons. These results support the suggestion that granitic (sensu lato; possibly TTGs) "proto-continental" crust existed by 4.3 Ga, although the amounts of such crust are still uncertain.

Summary

Zircons are highly retentive of primary magmatic $\delta^{18}O$ compositions. This is exemplified by uniform $\delta^{18}O$ values for all analyzed ocean-crust zircon grains, despite extensive subsolidus hydrothermal alteration of the host rocks. The narrow range in $\delta^{18}O$(Zrc) contrasts with large variations in whole-rock values that are caused by varying temperatures and extent of hydrothermal alteration. Magmatic zircons from plutonic ocean crust have average $\delta^{18}O = 5.2 \pm 0.5$‰, consistent with the range observed for zircons in high-temperature equilibrium with primitive mantle (5.3 ± 0.6‰; Valley et al. 2005). The $\delta^{18}O$(Zrc) data indicate that the magmas producing oceanic plagiogranite and differentiated Fe–Ti oxide gabbros beneath slow-spreading MOR did not carry a detectable seawater signature.

The $\delta^{18}O$(Zrc) data indicate that plagiogranites in slow-spreading environments form prior to significant interactions between the crust and seawater. If plagiogranites formed from hydrous partial melting of typical gabbros, the consistent, mantle-like $\delta^{18}O$(Zrc) indicates that the gabbros preserved MORB-like $\delta^{18}O$ at the time of melting. Thus, hydrothermal alteration of the gabbroic portions of ocean crust would have been limited to very low degrees of seawater–rock interaction prior to melting and zircon crystallization. Alternatively, the small amounts of water required for hydrous partial melting could have been magmatic in origin. The uniform $\delta^{18}O$(Zrc) for evolved MOR magmas provides a framework for interpreting the timing of significant subsolidus hydrothermal alteration of the gabbroic and plagiogranitic host rocks.

Contaminated magmas capable of producing zircons with $\delta^{18}O$ higher than the mantle-like value have not been observed at MOR spreading centers. Furthermore, altered (i.e., porous) ocean-crust zircons and late rims all yield $\delta^{18}O$(Zrc) values that are comparable to or lower than primitive mantle-like values. These results indicate that detrital or xenocrystic zircons within the rock record with $\delta^{18}O$ values greater than 6.0‰ are unlikely to have formed in this type of tectonic setting. This conclusion is critical for interpretations of Hadean detrital zircons, and argues against parent-magmas analogous to MOR plagiogranites.

Acknowledgments The authors gratefully acknowledge Noriko Kita for assistance and discussions during sample preparation, instrument tuning of the CAMECA IMS-1280, and data acquisition. We also thank Jim Kern for assistance maintaining the ion microprobe, John Fournelle for assistance on the SEM, and Brian Hess for expertise in sample mount preparation. Helpful conversations with Aaron Cavosie, and reviews from Jade Star Lackey and Wolfgang Bach are greatly appreciated. This research used samples from the Ocean Drilling Program and Integrated Ocean Drilling Program. Initial preparation of samples was funded by NSF (OCE-0352054, OCE-0752558, OCE-0550456). The present study was funded by NSF-EAR (0509639, 0838058) and DOE (93ER14389). The Wisc-SIMS Lab is partially funded by NSF-EAR (0319230, 0516725, 0744079).

References

Alt JC, Bach W (2006) Oxygen isotope composition of a section of lower oceanic crust, ODP Hole 735B. Geochem Geophys Geosyst 7:G12008. doi:10.1029/2006GC001385

Alt JC, Shanks WC, Bach W, Paulick H, Garrido CJ, Beaudoin G (2007) Hydrothermal alteration and microbial sulfate reduction in peridotites and gabbro exposed by detachment faulting at the Mid-Atlantic Ridge, 15°20′N (ODP Leg 209): a sulfur and oxygen isotope study. Geochem Geophys Geosyst 8:Q08002. doi:10.1029/2007GC001617

Bach W, Alt JC, Niu Y, Humphris SE, Erzinger J, Dick HJB (2001) The geochemical consequences of late-stage low-grade alteration of lower ocean crust at the SW Indian Ridge: results from ODP Hole 735B (Leg 176). Geochim Cosmochim Acta 65:3267–3287

Baines AG, Cheadle MJ, John BE, Grimes CB, Schwartz JJ, Wooden JL (2009) SHRIMP Pb/U zircon ages constrain gabbroic crustal accretion at Atlantis Bank on the ultraslow-spreading Southwest Indian Ridge. Earth Planet Sci Lett 287:540–550. doi:10.1016/j.epsl.2009.09.002

Bindeman IN, Valley JW (2002) Oxygen isotope study of the Long Valley magma system, California: isotope thermometry and convection in large silicic magma bodies. Contrib Mineral Petrol 144:185–205

Bindeman I, Gurenko A, Sigmarsson O, Chaussidon M (2008) Oxygen isotope heterogeneity and disequilibria of olivine crystals in large volume Holocene basalts from Iceland: evidence

for magmatic digestion and erosion of Pleistocene hyaloclastites. Geochim Cosmochim Acta 72:4397–4420. doi:10.1016/j.gca.2008.06.010

Blackman DK, Karson JA, Kelley DS, Cann JR, Fruh-Green GL, Gee JS, Hurst SD, John BE, Morgan J, Nooner SL, Ross DK, Schroeder TJ, Williams EA (2004) Geology of the Atlantis Massif (Mid-Atlantic Ridge, 30°N): implications for the evolution of an ultramafic oceanic core complex. Mar Geophys Res 23:443–469. doi:10.1023/B:MARI.0000018232.14085.75

Blackman DK, Ildefonse B, John BE, Ohara Y, Miller DJ, MacLeod CJ, Shipboard Scientists (2006) Proc Integr ODP, vol 304/305, College Station, TX. doi:10.2204/iodp.proc.304305.2006

Bosch D, Jamais M, Boudier F, Nicolas A, Dautria JM, Agrinier P (2004) Deep and high temperature hydrothermal circulation in the Oman ophiolite—petrological and isotopic evidence. J Petrol 45:1181–1208. doi:10.1093/petrology/egh010

Bouvier A, Ushikubo T, Kita N, Cavosie AJ, Kozdon R, Valley JW (2009) Li isotopes in Archean zircons. Eos Trans AGU 90(52) Fall Meet Suppl (abstract V14B-07)

Cann JR, Blackman DK, Smith DK, McAllister E, Janssen B, Mello S, Avgerinos E, Pascoe AR, Escartin J (1997) Corrugated slip surfaces formed at ridge-transform intersections on the Mid-Atlantic Ridge. Nature 385:329–332. doi:10.1038/385329a0

Cannat M (1996) How thick is the magmatic crust at slow spreading oceanic ridges? J Geophys Res 101:2847–2857

Cavosie AJ, Valley JW, Wilde SA EIMF (2005) Magmatic δ^{18}O in 4400–3900 Ma detrital zircons: a record of the alteration and recycling of crust in the Early Archean. Earth Planet Sci Lett 235:663–681

Cavosie AJ, Valley JW, Wilde SA, EIMF (2006) Correlated microanalysis of zircon: δ^{18}O and U-Th-Pb isotopic constraints on the igneous origin of complex >3900 Ma detrital grains. Geochim Cosmochim Acta 70:5601–5616. doi:10.1016/j.gca.2006.08.011

Cavosie AJ, Valley JW, Wilde SA (2007) The oldest terrestrial mineral record: a review of 4400 to 4000 Ma detrital zircons from the Jack Hills, Western Australia. In: MJ van Kranendonk, RH Smithies, VC Bennett (eds) Earth's oldest rocks. Dev Precambrian Geol 15:91–111

Cavosie AJ, Kita NT, Valley JW (2009) Mantle oxygen-isotope ratio recorded in magmatic zircon from the Mid-Atlantic Ridge. Am Mineral 9:926–934. doi:10.2138/am.2009.2982

Coleman RG, Donato MM (1979) Oceanic plagiogranite revisited. In: Barker F (ed) Trondhjemites, dacites, and related rocks. Elsevier, Amsterdam, pp 149–167

Coogan LA, Hinton RW (2006) Do the trace element compositions of detrital zircons require Hadean continental crust? Geology 34:633–636. doi:10.1130/G22737.1

Coogan LA, Wilson RN, Gillis KM, MacLeod CJ (2001) Near-solidus evolution of oceanic gabbros: insights from amphibole geochemistry. Geochim Cosmochim Acta 65:4339–4357. doi:10.1016/S0016-7037(01)00714-1

Crowley JL, Myers JS, Sylvester PJ, Cox RA (2005) Detrital zircon from the Jack Hills and Mount Narryer, Western Australia; evidence for diverse >4.0 Ga source rocks. J Geol 113:239–263. doi:0022-1376/2005/11303-0001

Delacour A, Früh-Green GL, Frank M, Gutjahr M, Kelley DS (2008) Sr- and Nd isotope geochemistry of the Atlantis Massif (30°N, MAR): Implications for fluid fluxes and lithospheric heterogeneity. Chem Geol 254:19–35. doi:10.1016/j.chemgeo.2008.05.018

deMartin BJ, Sohn RA, Canales JP, Humphris SE (2007) Kinematics and geometry of active detachment faulting beneath the trans-atlantic geotraverse (TAG) hydrothermal field on the Mid-Atlantic Ridge. Geology 35:711–714. doi:10.1130/G23718A.1

Dick HJB, Natland JH, Alt JC, Bach W et al (2000) A long in situ section of lower ocean crust: results of ODP Leg 176 drilling at the Southwest Indian Ridge. Earth Planet Sci Lett 179:31–51. doi:10.1016/S0012-821X(00)00102-3

Dixon JE, Stolper EM, Holloway JR (1995) An experimental study of water and carbon dioxide solubilities in mid-ocean ridge basaltic liquids. Part I: calibration and solubility models. J Petrol 36:1607–1631

Dixon-Spulber S, Rutherford MJ (1983) The origin of rhyolite and plagiogranite in oceanic crust: an experimental study. J Petrol 24:1–25

Eiler JM (2001) Oxygen isotope variations of basaltic lavas and upper mantle rocks. In: Valley JW, Cole DR (eds) Reviews in mineralogy and geochemistry, vol 43, pp 319–364

Eiler JM, Farley KA, Valley JW, Hofmann AW, Stolper EM (1996) Oxygen-isotope constraints on the sources of Hawaiian volcanism. Earth Planet Sci Lett 144:453–468

Farver JR (1989) Oxygen self-diffusion in diopside with application to cooling rate determinations. Earth Planet Sci Lett 117:407–422

Ferry JM, Watson EB (2007) New thermodynamic models and revised calibrations for the Ti-in-zircon and Zr-in-rutile thermometers. Contrib Mineral Petrol 154:429–437. doi:10.1007/s00410-007-0201-0

Fu B, Page FZ, Cavosie AJ, Fournelle J, Kita NT, Lackey JS, Wilde SA, Valley JW (2008) Ti-in-zircon thermometry: applications and limitations. Contrib Mineral Petrol 156:197–215. doi:10.1007/soo410-008-0281-5

Gaggero L, Cortesogno L (1997) Metamorphic evolution of oceanic gabbros: recrystallization from subsolidus to hydrothermal conditions in the MARK area (ODP Leg 153). Lithos 40:105–131

Gao Y, Hoefs J, Przybilla R, Snow JE (2006) A complete oxygen isotope profile through the lower oceanic crust, ODP Hole 735B. Chem Geol 233:217–234

Gillis KM (1995) Controls on hydrothermal alteration in a section of fast-spreading ocean crust. Earth Planet Sci Lett 134:473–489

Godard M, Awaji S, Hansen H, Hellebrand E, Brunelli D, Johnson K, Yamasaki T, Maeda J, Abratis M, Christie D, Kato Y, Mariet C, Rosner M (2009) Geochemistry of a long in situ section of intrusive slow-spread oceanic lithosphere: results from IODP Site U1309 (Atlantis Massif, 30°N Mid-Atlantic-Ridge). Earth Planet Sci Lett 279:110–122. doi:10.1016/j.epsl.2008.12.034

Gregory RT, Criss RE (1986) Isotopic exchange in open and closed systems. In: Valley JW, Taylor HP, O'Neil JR (eds) Reviews in mineralogy, vol 16, pp 91–127

Gregory RT, Taylor HP Jr (1981) An oxygen-isotope profile in a section of Cretaceous oceanic crust, Samail ophiolite, Oman: evidence for δ^{18}O buffering of the oceans by deep (>5 km) seawater-hydrothermal circulation at mid-ocean ridges. J Geophys Res 86:2737–2755

Grimes CB, John BE, Kelemen PB, Mazdab F, Wooden JL, Cheadle MJ, Hanghøj K, Schwartz JJ (2007) The trace element chemistry of zircons from oceanic crust: a method for distinguishing detrital zircon provenance. Geology 35:643–646. doi:10.1130/G23603A.1

Grimes CB, John BE, Cheadle MJ, Wooden JL (2008) Protracted construction of gabbroic crust at a slow-spreading ridge: Constraints from ^{206}Pb/^{238}U zircon ages from Atlantis Massif and IODP Hole U1309D (30°N MAR). Geochem Geophys Geosyst 9:Q08012. doi:10.1029/2008GC002063

Grimes CB, John BE, Cheadle MJ, Mazdab FK, Wooden JL, Swapp S, Schwartz JJ (2009) On the occurrence, trace element geochemistry, and crystallization history of zircon from in situ ocean lithosphere. Contrib Mineral Petrol 158:757–783. doi:10.1007/s00410-009-0409-2

Harrison TM (2009) The Hadean crust: evidence from >4 Ga zircons. Annu Rev Earth Planet Sci 37:479–505. doi:10.1146/annurev.earth.031208.100151

Harrison TM, Schmitt AK, McCulloch MT, Lovera OM (2008) Early (≥ 4.5 Ga) formation of terrestrial crust: Lu-Hf, $\delta^{18}O$, and Ti-thermometry results for Hadean zircons. Earth Planet Sci Lett 268:476–486. doi:10.1016/j.epsl.2008.02.011

Hart SR, Blusztajn JS, Dick HJB, Meyer PS, Muehlenbachs K (1999) The fingerprint of seawater circulation in a 500-meter section of ocean crust gabbros. Geochim Cosmochim Acta 63:4059–4080

Hofmann AE, Valley JW, Watson EB, Cavosie AJ, Eiler JM (2009) Sub-micron scale distributions of trace elements in zircon. Contrib Mineral Petrol. doi:10.1007/s00410-009-0385-6

John BE, Foster DA, Murphy JM, Cheadle MJ, Baines AG, Fanning M, Copeland P (2004) Determining the cooling history of in situ lower oceanic crust—Atlantis Bank, SW Indian Ridge. Earth Planet Sci Lett 222:145–160. doi:10.1016/j.epsl.2004.02.014

Jöns N, Bach W, Schroeder T (2009) Formation and alteration of plagiogranites in an ultramafic-hosted detachment fault at the Mid-Atlantic Ridge (ODP Leg 209). Contrib Mineral Petrol. doi:10.1007/s00410-008-0357-2

Karson JA (1998) Internal structure of oceanic lithosphere: a perspective from tectonic windows. In: Buck WR, Delaney PT, Karson JA, Lagabrielle Y (eds) Faulting and magmatism at mid-ocean ridges. AGU, Washington, DC, pp 177–218

Kelemen PB, Kikawa E, Miller DJ et al (2004) Proceedings of ODP initiative reports, vol 209. doi:10.2973/odp.proc.ir.209.2004

Kelley DS (1996) Methane-rich fluids in the oceanic crust. J Geophys Res 101:2943–2962

Kelley DS, Früh-Green GL (1999) Abiogenic methane in deep-seated mid-ocean ridge environments: Insights from stable isotope analyses. J Geophys Res 104:10439–10460

Kempton PD, Hawkesworth CJ, Fowler M (1991) Geochemistry and isotopic composition of Gabbros from Layer 3 of the Indian Ocean crust, Hole 735B. In: Von Herzen RP, Robinson PT (eds) Proceedings of ODP, Scientific Results, vol 118, pp 127–143

Kita NT, Ushikubo T, Fu B, Valley JW (2009) High precision SIMS oxygen isotope analyses and the effect of sample topography. Chem Geol 264:43–57. doi:10.1016/j.chemgeo.2009.02.012

Klein EM (2003) Geochemistry of the igneous oceanic crust. In: Rudnick RL (ed) The crust: treatise on geochemistry, vol 3. Pergamon, Oxford, pp 433–464

Koepke J, Feig ST, Snow J, Friese M (2004) Petrogenesis of oceanic plagiogranites by partial melting of gabbros: an experimental study. Contrib Mineral Petrol 146:414–432

Koepke J, Berndt J, Feig ST, Holtz F (2007) The formation of SiO_2-rich melts within deep oceanic crust by hydrous partial melting of gabbros. Contrib Mineral Petrol 153:67–84. doi:10.1007/s00410-006-0135-y

Lackey JS, Valley JW, Chen JH, Stockli DF (2008) Dynamic magma systems, crustal recycling, and alteration in the central Sierra Nevada Batholith: the oxygen isotope record. J Petrol 49:1397–1426. doi:10.1093/petrology/egn030

Lister CRB (1974) Penetration of water into hot rock. Geophys J Astron Soc 39:465–509

Maas R, Kinny PD, Williams IS, Froude DO, Compston W (1992) The Earth's oldest known crust: A geochronological and geochemical study of 3900–4200 Ma detrital zircons from Mt Narryer and Jack Hills, Western Australia. Geochim Cosmochim Acta 56:1281–1300. doi:10.1016/0016-7037(92)90062-N

Maeda J, Naslund HR, Jang YD, Kikama E, Tajima T, Blackburn WH (2002) High-temperature fluid migration within oceanic crust layer 3 gabbros: implications for the magmatic-hydrothermal transition at slow-spreading mid-ocean ridges. In Natland JH, Dick HJB, Miller DJ, Von Herzen RP (eds) Proceedings of the ODP, Scientific Results, vol 176. Ocean Drilling Program, College Station, pp 1–56

Manning C, Weston PE, Mahon KI (1996) Rapid high temperature metamorphism of the East pacific Rise gabbros at Hess Deep. Earth Planet Sci Lett 144:123–132

Manning CE, MacLeod CJ, Weston PE (2000) Lower-cracking front at fast-spreading ridges: evidence from the East Pacific Rise and the Oman ophiolite, in Ophiolites and oceanic crust: new insights from field studies and the Ocean Drilling Program. Spec Pap Geol Soc Am 349:261–272

Mattey D, Lowry D, Macpherson C (1994) Oxygen-isotope composition of mantle peridotite. Earth Planet Sci Lett 128:231–241

McCaig AM, Cliff RA, Escartin J, Fallick AE, MacLeod CJ (2007) Oceanic detachment faults focus very large volumes of black smoker fluids. Geology 35:935–938. doi:10.1130/G23657A.1

McCaig AM, Delacour A, Fallick AE, Castelain T, Früh-Green GL (2010) Detachment fault control on hydrothermal circulation systems: interpreting the subsurface beneath the TAG hydrothermal field using the isotopic and geological evolution of oceanic core complexes in the Atlantic. AGU Monograph, Washington DC (in press)

McCollom TM, Shock EL (1998) Fluid-rock interactions in the lower oceanic crust: thermodynamic models of hydrothermal alteration. J Geophys Res 103:547–575

Mével C, Cannat M (1991) Lithospheric stretching and hydrothermal processes in oceanic gabbros from slow spreading ridges. In: Peters T, Nicolas A, Coleman RG (eds) Ophiolite genesis and evolution of the oceanic lithosphere. Kluwer, Dordrecht, pp 293–312

Michael PJ, Cornell WC (1998) Influence of spreading rate and magma supply on crystallization beneath mid-ocean ridges: evidence from chlorine and major element chemistry of mid-ocean ridge basalts. J Geophys Res 103:18325–18356

Muehlenbachs K (1986) Alteration of the ocean crust and the ^{18}O history of seawater. In: Valley JW, Taylor HP, O'Neil JR (eds) Reviews in mineralogy, vol 16, pp 425–444

Muehlenbachs K, Byerly G (1982) ^{18}O-enrichments of silicic magmas caused by crystal fractionation at the Galapagos spreading center. Contrib Mineral Petrol 79:76–79

Natland JH, Dick HJB (2002) Stratigraphy and composition of gabbros drilled in Ocean Drilling Program Hole 735B, Southwest Indian Ridge: a synthesis of geochemical data. In Natland JH, Dick HJB, Miller DJ, Von Herzen RP (eds) Proceedings of the Ocean Drilling Program, Scientific Results, vol 176. Ocean Drilling Program, College Station, pp 1–69

Natland JH, Meyer PS, Dick HJB, Bloomer SH (1991) Magmatic oxides and sulfides in gabbroic rocks from Hole 735B and the later development of the liquid line of descent. In Von Herzen RP, Robinson PT, et al. (eds) Proceedings of the ODP, Scientific Results, vol 118. Ocean Drilling program, College Station, pp 75–111

Nehlig P (1993) Interactions between magma chambers and hydrothermal systems: oceanic and ophiolitic constraints. J Geophys Res 98:19621–19633

Nicolas A, Mainprice D (2005) Burst of high-temperature seawater injection throughout accreting oceanic crust: a case study in Oman ophiolite. Terra Nova 17:326–330. doi:10.1111/j.1365-3121.2005.00617.x

Nicolas A, Mainprice D, Boudier F (2003) High-temperature seawater circulation throughout crust of oceanic ridges: a model derived from the Oman ophiolites. J Geophys Res 108:2371–2391. doi:10.1029/2002JB002094

Niu Y, Gilmore T, Mackie S, Greig A, Bach W (2002) Mineral chemistry, whole-rock compositions, and petrogenesis of Leg 176 gabbros: data and discussion. Proc ODP Sci Results 176:1–60

Page FZ, Ushikubo T, Kita NT, Riciputi LR, Valley JW (2007a) High-precision oxygen isotope analysis of picogram samples reveals 2 μm gradients and slow diffusion in zircon. Am Mineral 92:1772–1775

Page FZ, Fu B, Kita NT, Fournelle J, Spicuzza MJ, Schulze DJ, Viljoen F, Basei MAS, Valley JW (2007b) Zircons from kimberlite: new insights from oxygen isotopes, trace elements, and Ti in zircon thermometry. Geochim Cosmochim Acta 71:3887–3903. doi:10.1016/j.gca.2007.04.031

Robinson PT, Erzinger J, Emmermann R (2002) The composition and origin of igneous and hydrothermal veins in the lower ocean crust—ODP Hole 735B, Southwest Indian Ridge. Proc ODP Sci Results 176:1–66. doi:10.2973/odp.proc.sr.176.019.2002

Rollinson H (2008) Ophiolitic trondhjemites: a possible analogue for Hadean felsic 'crust'. Terra Nova 20:364–369. doi:10.1111/j.1365-3121.2008.00829.x

Schroeder T, Cheadle MJ, Dick HJB, Faul U, Casey JF, Kelemen PB (2007) Nonvolcanic seafloor spreading and corner-flow rotation accommodated by extensional faulting at 15°N on the Mid-Atlantic Ridge: a structural synthesis of ODP Leg 209. Geochem Geophys Geosyst 8:Q06015. doi:10.1029/2006GC001567

Schwartz J, John BE, Cheadle MJ, Miranda E, Grimes CB, Wooden J, Dick HJB (2005) Inherited zircon and the magmatic construction of oceanic crust. Science 310:654–657. doi:10.1126/science.1116349

Singh SC, Crawford WC, Carton H, Seher T, Combier V, Cannat M, Canales JP, Düsünür D, Escartin J, Miranda JM (2006) Discovery of a magma chamber and faults beneath a Mid-Atlantic Ridge hydrothermal field. Nature 442:1029–1032. doi:10.1038/nature05105

Smith DK, Escartín J, Schouten H, Cann JR (2008) Fault rotation and core complex formation: significant processes in seafloor formation at slow-spreading mid-ocean ridges (Mid-Atlantic Ridge, 13°–15°N). Geochem Geophys Geosyst 9:Q03003. doi:10.1029/2007GC001699

Stakes D, Mével C, Cannat M, Chaput T (1991) Metamorphic stratigraphy of Hole 735B. In: Von Herzen RP, Robinson PT (eds) Proceedings of ODP Scientific Results, vol 118, pp 153–180

Taylor HP, Sheppard SMF (1986). Igneous rocks: I. processes of isotopic fractionation and isotope systematics. In: Valley JW, Taylor HP Jr, O'Neil JR (eds) Reviews in mineralogy, vol 16, pp 227–271

Trail D, Mojzsis SJ, Harrison TM, Schmitt AK, Watson EB, Young ED (2007) Constraints on Hadean zircon protoliths from oxygen isotopes, Ti-thermometry, and rare earth elements. Geochem Geophys Geosys 8:Q06014. doi:10.1029/2006GC001449

Tucholke BE, Lin J (1994) A geological model for the structure of ridge segments in slow spreading ocean crust. J Geophys Res 99:11937–11958

Tucholke BE, Lin J, Kleinrock MC (1998) Megamullions and mullion structure defining oceanic metamorphic core complexes on the Mid-Atlantic Ridge. J Geophys Res 103:9857–9866

Ushikubo T, Kita NT, Cavosie AJ, Wilde SA, Rudnick RL, Valley JW (2008) Lithium in Jack Hills zircons: evidence for extensive weathering of Earth's earliest crust. Earth Planet Sci Lett 272:666–676

Valley JW (2001) Stable isotope thermometry at high temperatures. In: Valley JW, Cole DR (eds) Reviews in mineralogy and geochemistry, vol 43, pp 365–413

Valley JW (2003) Oxygen isotopes in zircon. In: Hanchar JM, Hoskin PWO (eds) Reviews in mineralogy and geochemistry, vol 53, pp 343–385

Valley JW, Chiarenzelli JR, McLelland JM (1994) Oxygen isotope geochemistry of zircon. Earth Planet Sci Lett 126:187–206

Valley JW, Kinny PD, Schulze DJ, Spicuzza MJ (1998) Zircon megacrysts from kimberlite: oxygen isotope variability among mantle melts. Contrib Mineral Petrol 133:1–11

Valley JW, Peck WH, King EM, Wilde SA (2002) A cool early Earth. Geology 30:351–354

Valley JW, Lackey JS, Cavosie AJ, Clechenko CC, Spicuzza MJ, Basei MAS, Bindeman IN, Ferreira VP, Sial AN, King EM, Peck WH, Sinha AK, Wei CS (2005) 4.4 billion years of crustal maturation. Contrib Mineral Petrol 150:561–580. doi:10.1007/s00410-005-0025-8

Vanko DA, Stakes DS (1991) Fluids in oceanic layer 3: evidence from veined rocks, Hole 735B, Southwest Indian Ridge. In Von Herzen RP, Robinson PT (eds) Proceedings of ODP, Scientific Results, vol 118, pp 181–215

Watson EB, Harrison TM (2005) Zircon thermometer reveals minimum melting conditions on earliest Earth. Science 308:841–844. doi:10.1126/science.1110873